Progress Report No. 1
ODOT Study No. 79-09-2
ORA 153-867

STRENGTH CHARACTERISTICS OF THE STABILIZED BOGGY SHALE

Prepared for
OKLAHOMA DEPARTMENT OF TRANSPORTATION
Oklahoma City, Oklahoma

Prepared by
George A. Lazaris, Graduate Research Assistant
Joakim G. Laguros, Professor
School of Civil Engineering and Environmental Science
The University of Oklahoma

Norman, Oklahoma
November 8, 1979

SUMMARY

In cooperation with the Oklahoma Department of Transportation and the Federal Highway Administration, U.S. Department of Transportation, a research project entitled "Field Application of the Stabilization of Oklahoma Shales" (ODOT Study 79-09-2, ORA 158-867) was undertaken on June 1, 1979 by the University of Oklahoma.

Initially, the Boggy shale in Atoka County was selected to be field stabilized. Later on, however, and because of seasonal limitations imposed on construction this site was abandoned for another site west of Enid. The laboratory work envisioned in Phase I had progressed to the point that it was considered prudent to continue and complete this effort. This Progress Report No. 1 presents the findings of this laboratory work.

The stabilizing agents used were 12% portland cement, 5% hydrated lime, and 25% fly ash. The curing conditions were 28 days moist curing at 70°F and 100°F, and two compaction conditions were employed: no delay and 2 hours delay. The effectiveness of stabilization was evaluated in terms of the shear strength parameters of cohesion and internal angle of friction determined through triaxial compressive and direct shear strength tests as well as plasticity.

Cement stabilization imparted maximum strength gain into shale with lime and fly ash giving lower but adequate strengths. Higher temperatures, namely 110°F, increased the effectiveness of stabilization but delayed compaction tended to slightly decrease it.

TABLE OF CONTENTS

TABLE OF CONTENTS (continued)

LIST OF TABLES

LIST OF TABLES (continued)

LIST OF FIGURES

LIST OF FIGURES (continued)

STRENGTH CHARACTERISTICS OF THE STABILIZED BOGGY SHALE

CHAPTER I

INTRODUCTION

Highway engineers have been experiencing numerous problems with cohesive soils and shales in highway construction. In Oklahoma, shale is abundant and it has been observed that it undergoes changes in plastic properties when it is exposed to the weathering action and to loads induced by traffic during its service life. The wide range of shale types and the problems associated with the field performance of these materials, triggered extensive studies at the University of Oklahoma. Laguros (1972) classified and identified shales using, as a basis, its engineering properties. This extensive study encompassed approximately 40 different shales sampled from various geographical locations in Oklahoma. As a result of this study, shales were grouped into eight classes with one shale from each class identified as a representative of that class. More recently, Laguros and Jha (1977), studied, in the laboratory, the performance of the so-selected eight shales stabilized using as stabilizing agents lime, portland cement, flyash, and chlorides of sodium and calcium.

The primary objective of this investigation was to ameliorate shale properties and upgrade the substandard shale material. Of the recommendations made at the conclusion of this study the most pertinent and significant was the need for field study and implementation.

To effect this recommendation it was proposed that a study site be selected using as general criteria of selection the following: a) a location where a problem shale was encountered, b) a road where sampling and/or testing could be carried out without extensive interference from traffic, and c) a road where traffic volume was commensurate with the limited function of the stabilized road. Care was to be taken to locate the entire length of the test road on a cut section, stabilize the entire width of the road and, if possible, to have the test road on the same grade throughout.

The field implementation includes the following phases:

Phase I: Design

Phase II: Construction

Phase III: Collection of field data

Phase IV: Analysis of data.

The purpose of the present investigation was to carry out part of Phase I which included: a) sampling of shale and b) laboratory testing to determine the engineering properties (gradation, atterberg limits, and optimum moisture content - dry density). As an extension, the study

encompassed the determination of the two shear strength parameters, namely, the cohesion, c, and angle of internal friction, ϕ, of the selected shale stabilized separately with lime, portland cement, and flyash. These parameters were calculated from triaxial and direct shear test data and an attempt has been made to correlate the values of c and ϕ obtained from the two testing procedures.

CHAPTER II

STABILIZATION IN GENERAL

"Soil stabilization is the collective term for any physical, chemical, or biological method, or any combination of such methods, employed to improve certain properties of a natural soil to make it serve adequately an intended engineering purpose" (Winterkorn and Fang, 1975). Although modern soil stabilization, as known today in highway and airport construction, is an art of relatively recent origin, the fundamental principles upon which it rests have been known and practiced for a long time. During the ancient Greek civilizations of Athens, Crete, and Skyros for example, streets were constructed of large blocks cemented together with "santor" (a volcanic turfaceous agglomerate from the isle of Santorin), earth, lime, and water. The Roman roads outlasted the Empire, and the Appian Way is often referred to as the first lime-stabilized road.

Stabilization is usually mechanical or chemical, but occasionally thermal and electrical means have been used. Mechanical stabilization includes compaction, blasting, and various patented vibration techniques. Chemical stabilization includes the mixing or injecting of chemical substances

into the ground. Such chemical substances are: lime, portland cement, sodium chloride, calcium chloride, flyash, and asphalt.

Based on the mechanisms that take place when they are incorporated into the soil, the stabilizing agents may be grouped into two major categories: the "active" and the "inert" (ASCE, 1978). The "active" stabilizers produce chemical reactions with the soil, which in turn cause desirable changes in engineering characteristics of the soil. The chemical properties of the soil such as, presence of organic matter, predominant type of clay mineral, natural soil pH and to a certain extent, texture and plasticity, are very important. With "inert" stabilizers, which do not react chemically with the soil or aggregate stabilization is achieved as a result of bonding among particles. This increases the shearing strength of the soil aggregate mixture. Stabilization is also achieved by improvement of the water-proofing characteristics of the soil. An example of this type of stabilizer is bituminous material. The physical characteristics of soil, such as texture and gradation, assume great importance in this type of stabilization. Many stabilizers such as lime, flyash, and portland cement display both the active and the inert characteristics, thus necessitating the consideration of the chemical, as well as the physical soil properties in a stabilization study.

There are many stabilizing agents available in the market today but they are not suitable for large scale use

for various reasons, one of which is cost. The three important chemically active stabilizing agents presently in use are lime, flyash, and portland cement.

Lime Stabilization

Lime, as a soil additive, brings several beneficial changes to soils containing silt and clay particles. The National Lime Association (NLA, 1954) reports that the addition of lime to wet soils dries them out and improves their workability. Davidson and Handy (1959) report that with the addition of lime, calcium ions cause a reduction in the plasticity of cohesive soils rendering them more friable and more workable. The mechanism which causes this, is either a cation exchange or a crowding of additional cations onto clay platelets. Both these processes change the electrical charge around the clay particles. Clay particles, then, become electrically attracted to one another causing flocculation or aggregation. The change in the electrical charge also increases the porewater pH which, in turn, makes alumina and silica more soluble and simultaneously the calcium ions react with hydrous alumina to form hydrated calcium aluminate (Diamond and Kinter, 1966). This rather fast reaction supplemented by a slower reaction of silica with lime, generates hydrated calcium silicate better known as "tobermorite gel" ($3CaO \cdot 2SiO_2 \cdot 3H_2O$). The gradual hardening of the gel imparts strength to the soil lime mix.

During the initial stage, at the points of contact between the edges of one particle and the forces of adjacent particles, very small quantities of cementing products are formed. The formation of the cementing product is believed to be sufficient to stabilize the flocs with the result that the index properties are modified. The bonding among the flocs, however, is not at level to provide sufficient strength to the soil mass and the clay seems to be ameliorated but not stabilized. Compaction to minimum void ratio is essential to stabilize the mix.

The mechanism of lime stabilization of clay soils is presented in Figure 2.1. A simplified qualitative view of some typical soil lime reactions is summarized below:

$$Ca(OH)_2 \longrightarrow Ca^{++} + 2(OH)$$

$$Ca^{++} + 2(OH)^- + SiO_2 \text{(clay silica)} \longrightarrow CSH$$

$$Ca^{++} + 2(OH)^- + Al_2O_3 \text{(clay alumina)} \longrightarrow CAH$$

Depending on such factors as, reaction conditions, quantity and type of lime, soil characteristics, curing time, and temperature, a wide variety of hydrated forms can be obtained.

Some typical soil lime reactions are:

Kaolinite + lime $\longrightarrow$ CSH(C/S = 0.2-1)
+ CAH + CASH . . . . . .(Moh, 1965)

Kaolinite + lime $\longrightarrow$ CASH(Prehnite) . . . (Sloane, 1965)

Montmorillonite + lime $\longrightarrow$ CSH(gel) + CSH(1)
+ tobermorite + hydrogarnet

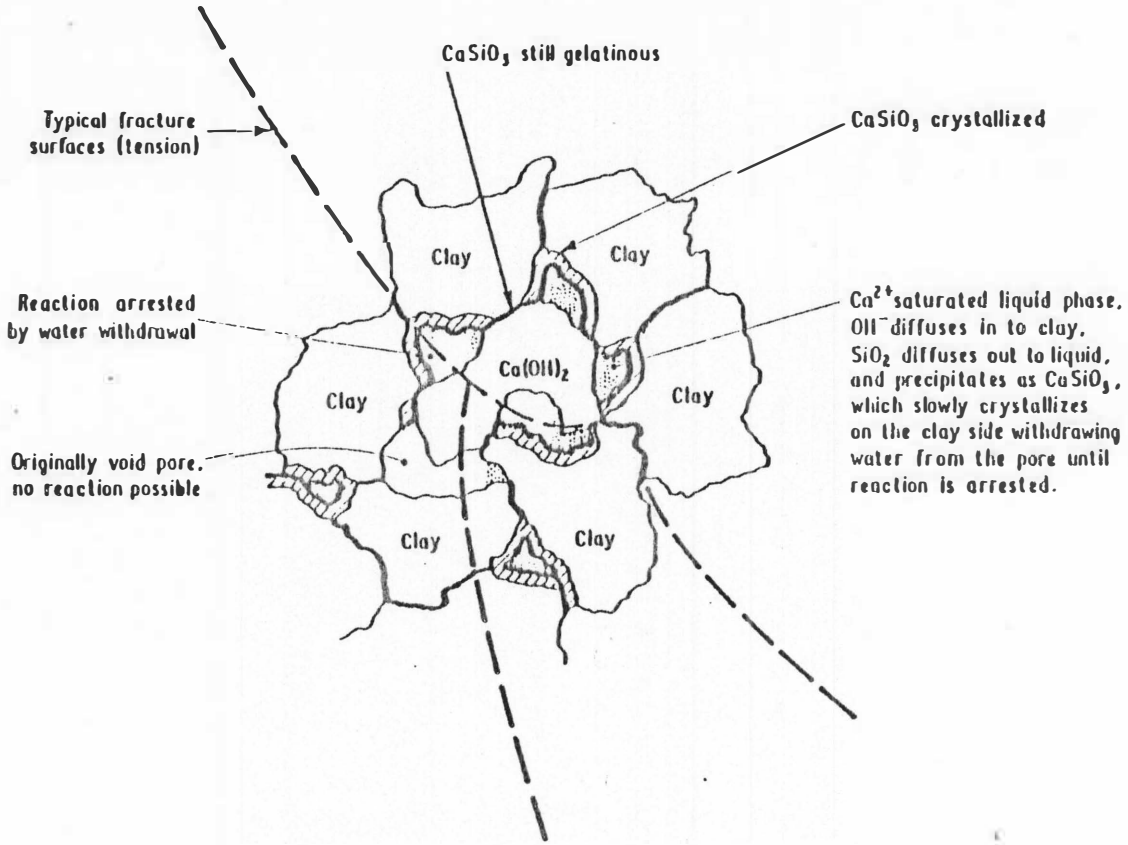

Figure 2.1 Mechanism of lime stabilization of clay soils (After Ingles, 1970).

Clay + lime $\longrightarrow$ CSH(gel) and/or CSH(l)

+ C_4AH_{13} + C_3AH_6 . . . . . (Diamond, White, and Dolch, 1964)

Montmorillonite + lime $\longrightarrow$ CSH + hydrogarnet

- C_4AH_{13} . . . . . (Wang and Handy, 1966)

where,

C = Calcium Oxide, CaO

S = Silicon Dioxide, SiO_2

A = Aluminum Oxide, Al_2O_3

H = Water, H_2O.

In summary, the addition of lime changes the physical characteristics of most clay soils. Wang and Handy (1966) summarized these physical changes as follows:

1. Decrease in plasticity index, decrease in liquid limit and increase in plastic limit.
2. Decrease in shrinkage and swell.
3. Increase in friability and workability of soil due to the disintegration of soil aggregated during pulverization.
4. Decrease in soil binder content.
5. Increase in compressive strength.
6. Drying of soil.

These modifications make lime an excellent stabilizing agent for construction of highway bases and subbases wherever clayey soils are encountered.

Cement Stabilization

Portland cement finds extensive use as a soil stabilizing agent. The correct proportion of cement to soil is determined in the laboratory. The American Builders Association recommends the following testing:

1. Testing required to classify the soil according to the classification system of the Federal Highway Administration.
2. The determination of "Optimum Moisture Content" (OMC) and "Maximum Dry Density" of trial mixtures with different proportions of cement to soil.
3. Preparation of two sets of specimens molded at the optimum moisture content from each of the trial mixtures. One set of specimens from each trial mixture is then subjected to wetting and drying cycles while the other is subjected to freeze-thaw cycles (12 cycles, ASTM method).

The amount of portland cement which is required to produce an acceptable mixture is determined by comparing the amount of losses during each cycle of testing.

The various effects of portland cement stabilization include:

1. Plasticity reduction. Addition of cement to moist cohesive soils brings a considerable reduction in plasticity due to the release of calcium ions during the initial hydration reaction (Jha, 1977).

As with the lime stabilization, the mechanism is either a crowding of the existing cations along with the additional cations or a cation exchange. These processes change the electrical charge around the clay particles and particles become attracted to one another. The electrical attraction of the clay particles causes flocculation and aggregation which in turn forces particles to behave like silt with low plasticity and cohesion. Addition of even relatively low amounts of portland cement causes immediate aggregation of particles.

2. Cementation. The early and the long term strength gains in compacted portland cement treated soil is attributed to the cementitious amorphous and crystalline hydration products of the different cement constituents (Jha, 1977). The cementation process may be visualized as being due to the development of chemical bonds or linkages between adjacent cement grain surfaces and between the cement grain surfaces and the exposed soil particle surfaces.
3. Fine grained soils. In fine grained soils the hydrated cement develops strong linkages between the mineral aggregates and the soil aggregates to form a matrix that encases the soil aggregates and is effective in fixing the particles so they can no longer slide over each other. Thus, the shear strength of soil is markedly increased.

4. Granular soil. In granular soils, stabilization causes cementation which takes place only at the points of contact of the aggregates. Therefore, for a well compacted sandy material and due to small void volume, the contacts are much longer and the cementing action stronger. For uniformly graded sand the contact area between the particles is minimum and for stabilization purposes the cement requirement is higher.

The mechanism, by which a rather small amount of portland cement can change the properties of a large mass of soil is still not completely defined, but various suggestions have been made. One suggestion is that the cement forms strong nuclei distributed throughout the voids in such a manner as to restrain the unaffected soil (Davidson, 1962). Another suggestion is that in a montmorillonite clay, the stress strain behavior supports a nucleated structure at low cement contents. As the cement content increases, this structure changes to a skeleton type structure and the nuclei grow into each other as a result of a secondary cementation process (Herzog, 1963). Ordinary portland cement consists mainly of about 45% tricalcium silicate (C_3S) and approximately 27% dicalcium silicate (C_2S). Since it hydrates in the presence of soil to form gels of mono- and dicalcium silicate hydrate (CSH and C_2SH), the reactions that take place may be presented as:

$C_3S + 2H = C_2SH + CH$

$C_2S + 2H = CSH + CH$

Some free lime (CH) is liberated in the hydration reaction. Laguros (1962) has presented, schematically, the process of setting, hardening and aging in terms of the physical systems and conditions in a form of a process diagram (Figure 2.2).

Flyash Stabilization

Flyash is the fine residue from burning of powdered coal, collected in the stacks of power plants by electrical precipitators or mechanical means, or combination of the two. It consists mainly of solid or hollow spherical particles of siliceous and aluminous glass, with small proportions of thin-walled, multi-faced polyhedrous called "cenospheres." Also, it consists of porous or carbon-coated particles high in iron and irregular in shape (Morgan, 1952).

The rapid growth in the use of powdered coal led to the increasingly restrictive regulations against discharge of smoke, particularly in densely populated areas. For each ton of powdered coal burned, from 160 to 280 pounds of flyash are produced; which indicates the magnitude of the problem.

Nowadays, flyash finds extensive use as a stabilizing agent in highway construction. It is used as the main stabilizing agent or in combination with lime, portland cement or other additives and it functions as a "pozzolan."

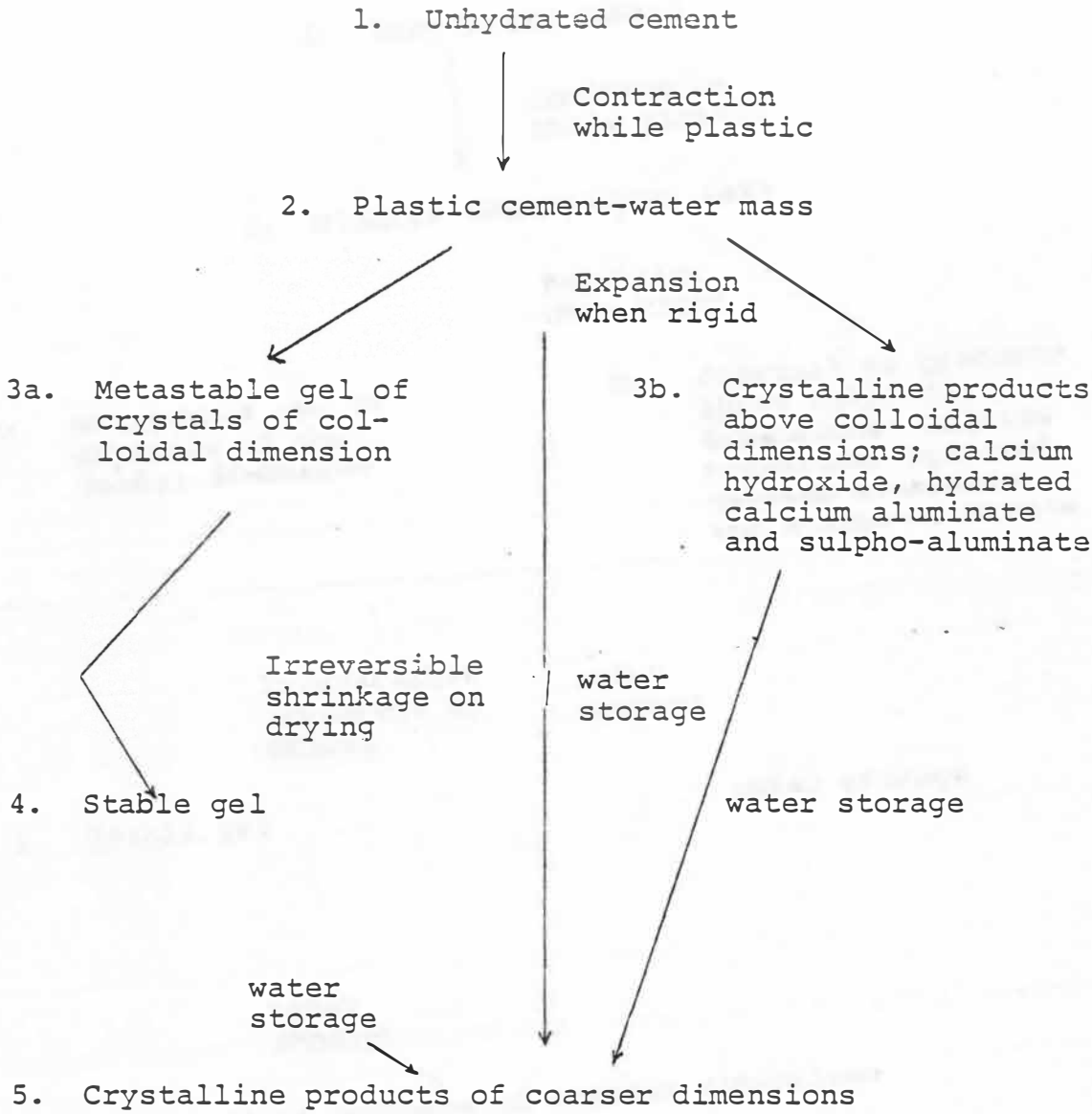

Figure 2.2. Process diagram for cement setting hardening and aging (Laguros, 1962).

Pozzolans may be defined as siliceous or siliceous and aluminous material (low in lime content) which posses in themselves little or no cementitious properties, but which in finely divided form will, in the presence of moisture, react chemically with calcium hydroxide, at ordinary temperatures, to form insoluble compounds possessing cementitious properties (ASTM, 1958).

The reactions that occur in the lime flyash system are complex. Minnick (1967) presents a list of reactions as follows:

1. $RO \xrightarrow{H_2O} R(OH)^2$
2. $RO \xrightarrow{H_2O \cdot CO_3} R\,CO_3 + H_2O$
3. $R(OH)_2 \xrightarrow{CO_2} R\,CO_3 + H_2O$
4. $R(OH)_2 + SiO_2 \xrightarrow{H_2O} xR\,O \cdot ySiO_2 \cdot zH_2O$
5. $R(OH)_2 + Al_2O_3 \xrightarrow{H_2O} xR\,O \cdot yAl_2O_3 \cdot zH_2O$
6. $R(OH)_2 + Al_2O_3 + SiO_2 \xrightarrow{H_2O} xR\,O \cdot yAl_2O_3 \cdot zSiO_2 \cdot wH_2O$
7. $R(OH)_2 + SO_3^{--} + Al_2O_3 \xrightarrow{H_2O} xR\,O \cdot yAl_2O_3 \cdot zRSO_4 \cdot wH_2O$

where,

R = Ca

x, y, z, w = prefixes to balance the equations.

There is, however, a possibility of other reactions occurring.

Shearing Strength of Soils

The shear strength of a soil may be attributed to a combination of physical factors and physico-chemical factors. The physical components of shear strength are customarily attributed to frictional resistance (i.e., the resistance to

sliding of one surface on another) and to interlocking between particles. Rosenquist (1959) divided interlocking into two parts: a) a large scale interlocking between the particles which requires considerable movements of particles normal to the shear plane for failure to occur and b) a small scale interlocking due to particle surface roughness, requiring only small movements normal to the shear plane in order that failure might occur. These physical factors are proportional to the effective normal stress on the failure plane, and are significant in the granular particles (Seed, Mitchell, and Chen, 1960).

A second component of soil strength is attributed to the physico-chemical conditions in the soil and is often referred to as "cohesion." Cohesion in a soil is that part of the soil strength which is present independently of any applied pressures, either mechanical or capillary, and would remain if all applied pressures were removed. Cohesion is the bonding of particles within a soil mass by physico-chemical mechanisms of an interatonic, intermolecular or interparticle nature. In a typical cohesive soil containing granular and clay size particles, the total strength will be the sum of the contributions of each of the components. Values of cohesion and interparticle friction vary for different types of soils. For a given normally consolidated soil, for example, the undrained strength should increase linearly with overburden stress and hence linearly

with depth. Bjerrum (1954), reports a shear strength as low as 4.5 psi, for a Norwegian marine clay. On the other hand, Skempton and Henkel (1957) for the shear strength of a London clay a value of 41.0 psi. Sandy soils show a high value for the angle of internal friction while cohesion is zero.

CHAPTER III

SELECTION OF MATERIALS

Laguros (1972) identified the areas of problem shales in Oklahoma. Kumar and Laguros (1974) and Laguros and Jha (1977) have studied the amenabilities of Oklahoma shales to various additives for stabilization.

Based on these studies and for purposes of field implementation a section of State Highway 131 was selected. It is located in Atoka County west of U.S. Highway 69 as shown in Figure 3.1. The details of the shale encountered on this highway are given in Table 3.1.

The stabilizing agents used were lime, portland cement, and flyash. Hereafter, the symbols L, PC, and FA will be used to identify lime, portland cement, and flyash, respectively.

The hydrated lime used was manufactured by the Austin White Lime Co., Austin, Texas. To prevent carbonation of the lime, individual one pound bottles were kept sealed until immediately before use. The maximum amount of impurities for this lime are presented in Table 3.2.

The portland cement Type I used was supplied by Ideal Basic Industries, Denver, Colorado, and its chemical composition is presented in Table 3.3.

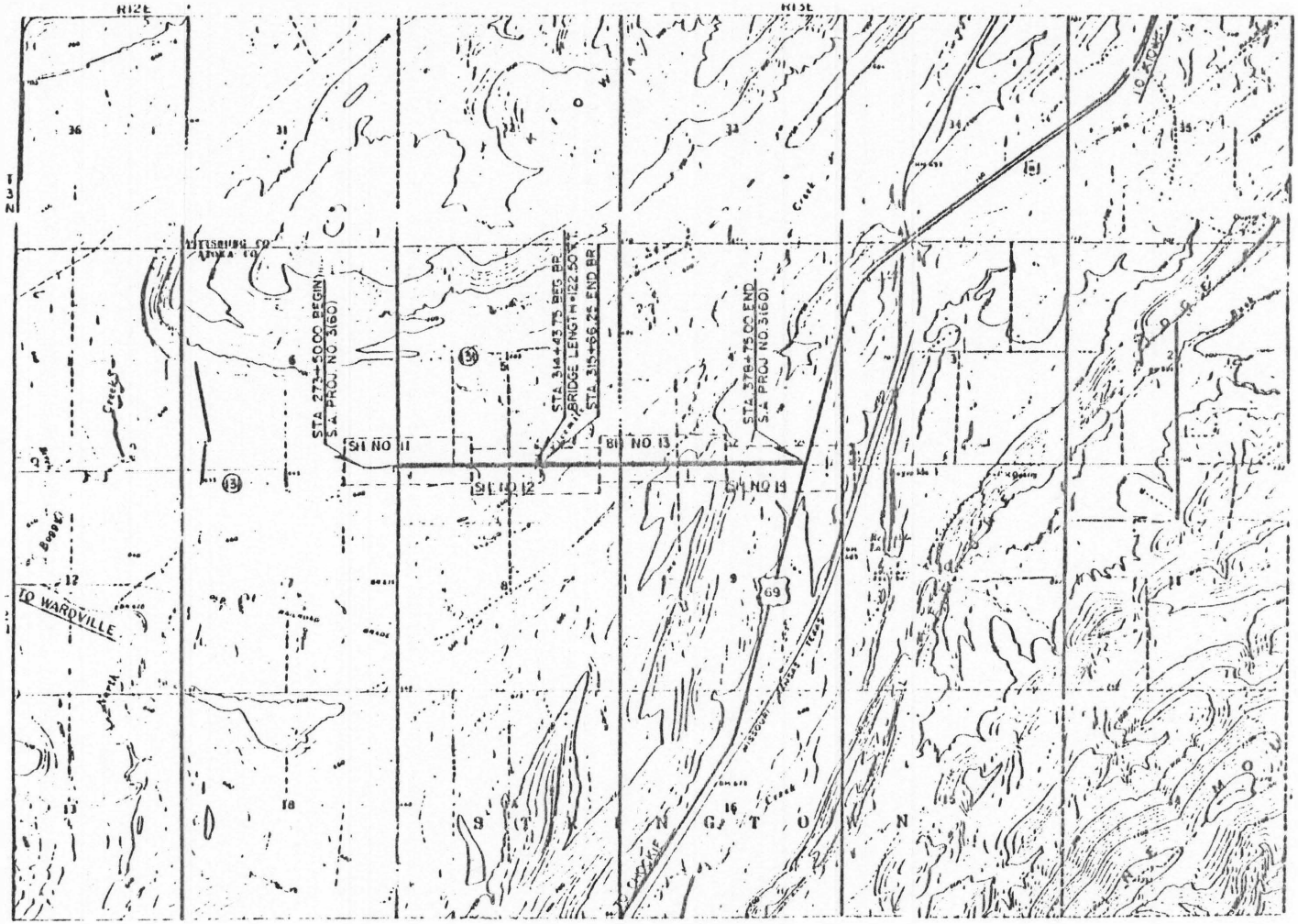

Figure 3.1 Location of sampling site.

TABLE 3.1

DESCRIPTION OF SHALE

Geological unit	Boggy
County	Atoka
Sampling location	Section of State Hwy 131 East of Hwy 9
Field description	Brown to gray silty clay
AASHTO classification	A-7-6(6)
Sand, %	12
Silt, %	51
Clay (<2μ), %	35
Liquid limit, %	36
Plasticity index	25

TABLE 3.2

IMPURITIES OF LIME MANUFACTURED BY THE
AUSTIN WHITE LIME COMPANY, AUSTIN, TEXAS

Silicon Dioxide	0.10
Iron Oxide	0.30
Titanium Oxide	0.01
Manganese Dioxide	0.01
Aluminum Oxide	0.20
Calcium Oxide	70.98
Mangnesium Oxide	0.58
Sulfur Trioxide	Less than 0.01
Phosphorous Pentoxide	Less than 0.01
Carbon Dioxide	5.35
Chemically combined moisture	19.31

TABLE 3.3

CHEMICAL COMPOSITION OF TYPE I PORTLAND CEMENT MANUFACTURED BY IDEAL BASIC INDUSTRIES, DENVER, COLORADO

SiO_2	20.9
Al_2O_3	5.2
Fe_2O_3	2.8
CaO	64.2
MgO	2.0
SO_3	3.1
Na_2O	0.19
K_2O	0.68
Loss	0.9

The flyash used in this study was supplied by the Muskogee Environmental Conservation Company, Muskogee, Oklahoma. Its anticipated chemical analysis is presented in Table 3.4.

TABLE 3.4

ANTICIPATED MINERAL ANALYSIS OF ASH FROM OKLAHOMA GAS AND ELECTRIC COMPANY, MUSKOGEE, OKLAHOMA

Silica, SiO_2	36.23
Aluminum Oxide, Al_2O_3	19.03
Ferric Oxide, Fe_2O_3	9.72
Sulphur Trioxide, SO_3	2.62
Calcium Oxide, CaO	26.25
Magnesium Oxide, MgO	4.94
Avail. Alkalines, (Na_2O)	1.20

CHAPTER IV

TESTING PROCEDURE

The samples obtained from the field were air dried and then ground to pass U.S. Standard Sieve No. 10. Preliminary shale identifications tests employed in this study are: a) grain size analysis, b) Atterberg limits, and c) moisture density tests. Distilled water was used in all experiments conducted under this study.

Grain Size Analysis

The grain size distribution of the shale was determined in accordance with the AASHTO Designation T88-78 (ASTM designation D422-63) with the exception that the Iowa jet dispersion apparatus was used at an air-pressure of 10 psi for about five minutes. Prior to dispersion the shale was ultrasonically treated for one hour to provide improved design criteria (Laguros, 1972). The ultrasonic apparatus used is shown in Figure 4.1.

Atterberg Limits

The liquid limit and the plastic limit tests were run in accordance with the AASHTO Designation T89-76 (ASTM

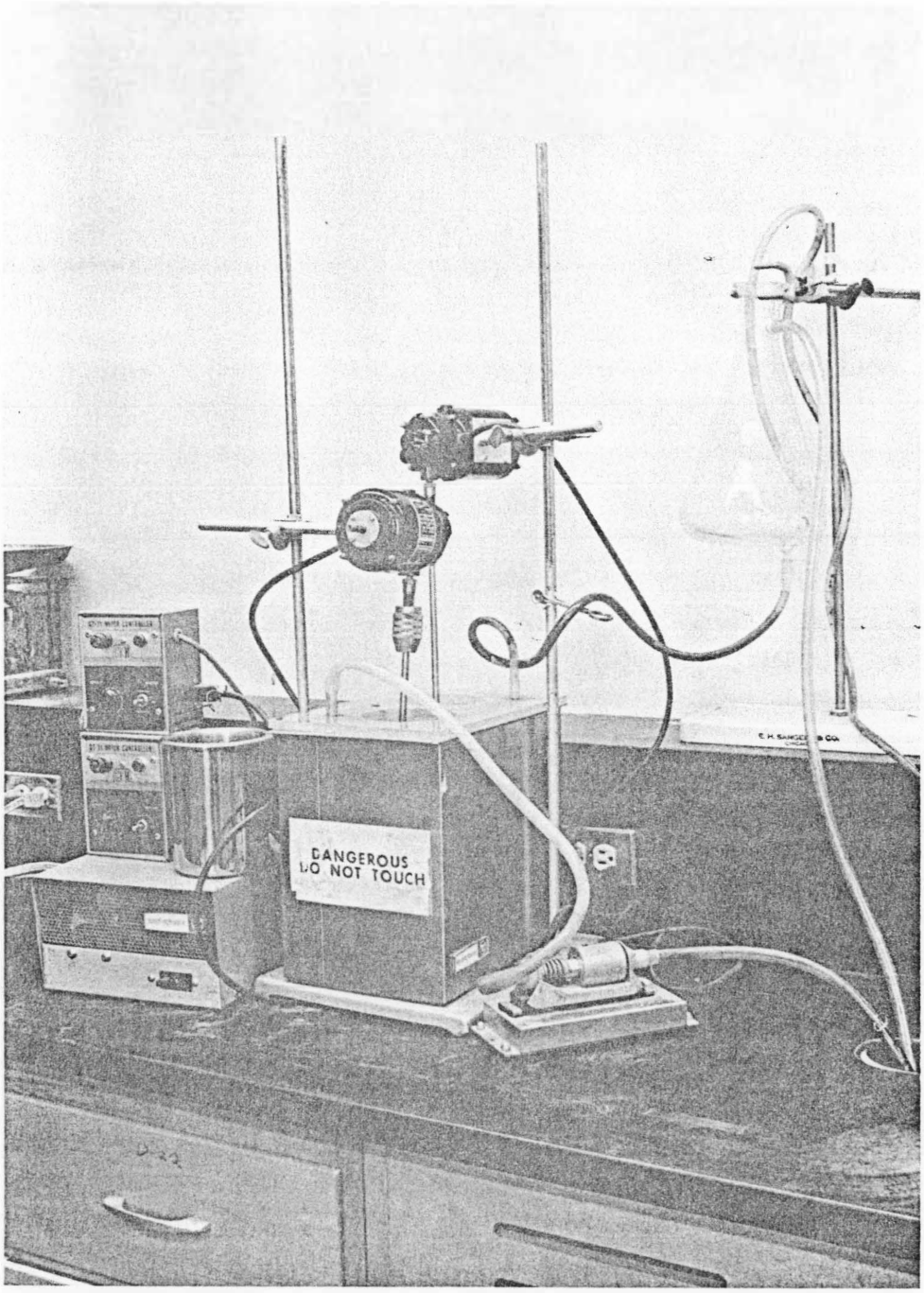

Figure 4.1 General view of ultrasonic equipment and water circulating system.

designation D423-66) and the AASHTO Designation T90-70 (ASTM D424-65), respectively.

Moisture Density Relationships

For the raw and stabilized shale mixes moisture density relationships were determined using the Harvard Miniature Compaction procedure which gives near Standard Proctor results. The samples were compacted in five layers under a compactive effort of 25 blows per layer, using a 20 lb spring loaded rammer. The main advantage in using the Harvard method is that it requires only 1.5 lb of sample in contrast to about 15 lbs required for the Standard Proctor test. The values of maximum dry density and corresponding optimum moisture content for the raw shale and the stabilized shale mixes are given in Table 4.1.

Preparation of Samples for Strength Testing

Triaxial Testing Samples

Air dried portions of shale passing U.S. Standard Sieve No. 10 were used for sample preparation. The hygroscopic moisture content was determined in order to make the necessary adjustments for calculating the amounts of additives or additional molding water. The stabilizing agent was added and the mix was thoroughly blended by hand. Distilled water was then added in an amount required for achieving OMC. The mixture was again thoroughly mixed by hand. The mix which was designated for the 2-hr delayed

TABLE 4.1

MAXIMUM DRY DENSITY AND OPTIMUM MOISTURE CONTENT OF RAW SHALE AND SHALE ADDITIVE MIX

Type of Shale	DD, pcf[a]	OMC, %[b]
Raw shale	113.2	14.2
Shale + 5%L	106.8	19.0
Shale + 12%PC	110.0	16.0
Shale + 25%FA	116.2	14.0

[a] Maximum dry density

[b] Optimum moisture content

compaction was prepared in the same manner and sealed in Saran Wrap to prevent moisture evaporation until compaction. Samples for triaxial shear tests were statically compacted in the apparatus shown in Figure 4.2.

Samples prepared in this apparatus were 1.35 inches in diameter and 2.95 inches in height. The volume of the sample prepared by this apparatus is ten percent greater than that of the sample obtained from the Harvard miniature compaction apparatus. The calculated volume of the mix was carefully poured into the molding tube, and along with the top and bottom plungers it was placed under a compression machine until the flanges of the plungers were in contact with the ends of the tube. This assembly was left under pressure for about five minutes. The load was then removed and the plungers withdrawn. The sample was extracted from the tube using an extraction plunger by means of a hydraulic jack. The extracted samples were weighed, wrapped in Saran Wrap and stored in the humidifier. The samples were cured for 28 days at 90 to 100% relative humidity and at two different temperatures: one at 70°F and the other at 110°F. At the end of the curing period, the samples were removed from the humidifier, unwrapped, weighed, their dimensions measured, and then tested for triaxial shear strength. The samples tested in the soaked condition, were unwrapped and immersed in water for 12 hours at the end of the curing period. Following the immersion, the samples were weighed and then tested similarly to the dry ones.

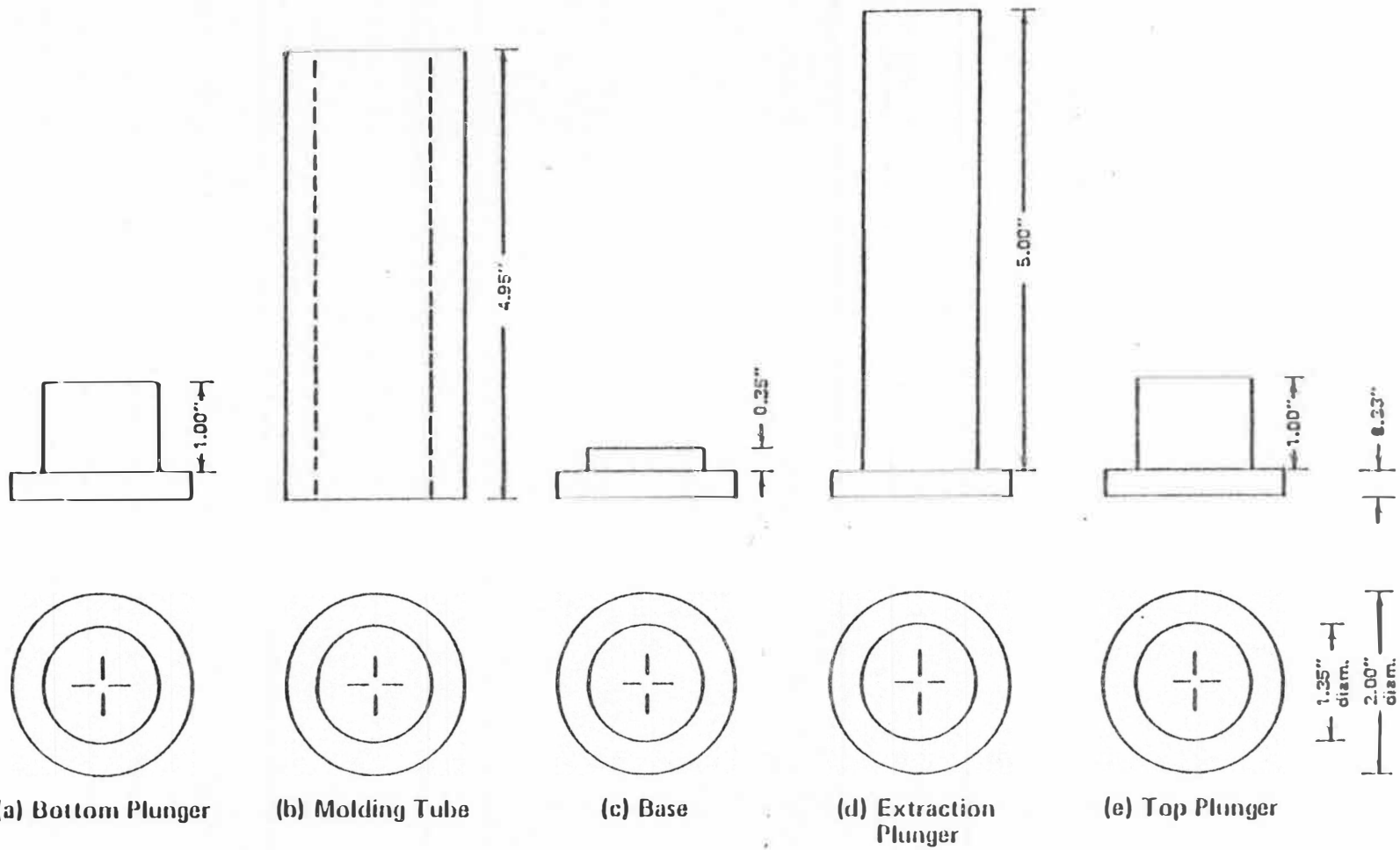

Figure 4.2 Details of sample molding apparatus.

Direct Shear Testing Samples

Samples for direct shear testing were prepared in a manner similar to AASHTO Designation T99-74 (ASTM Designation D698-64T). Amounts of shale, stabilizing agent(s), and distilled water required for maximum dry density and optimum moisture content were weighed and thoroughly mixed together. The mix, weighing approximately 2.5 kgs, was poured into the cylindrical mold and the samples were compacted in three layers under a compactive effort of 25 blows per layer, using a manually operated 5.5 kg rammer dropped from a height of 12 inches. The sample was extracted from the molding tube by means of a hydraulic jack. Using an electric saw, the sample was cut into three sections of approximately 1.5 inches in height and trimmed to about 2.25 inches in diameter. The so-prepared samples were wrapped in Saran Wrap and aluminum foil, labeled and stored in the humidifier. At the end of the curing period, the samples were removed from the humidifier, unwrapped, and trimmed down by hand to two inches in diameter. The sample was then carefully placed in the test ring. The surface irregularities, if any, were filled with material passing U.S. Sieve No. 200. The assembly was then placed in the direct shear machine. Samples prepared for testing in the soaked condition were unwrapped and immersed in water for 12 hours. At the end of the curing period the samples were tested in a manner similar to that described for dry samples.

Strength Testing

Triaxial Shear Strength Test

In the conventional method of triaxial shear strength test, the sample is loaded to failure by increasing the axial stress while holding the confining stress constant. The confining pressure is applied by either air or liquid under pressure. The triaxial shear test gives an accurate measure of the shear strength for both cohesionless and cohesive soils.

The general Mohr-Coulomb failure law is expressed by the formula:

$$\tau = \bar{c} + \sigma \tan\phi \qquad (4.1)$$

where,

τ = shear stress

c = cohesion

σ = total normal stress

ϕ = angle of internal friction.

In terms of the effective stress, the Mohr-Coulomb equation is written as:

$$s = \bar{c} + \bar{\sigma} \tan\bar{\phi} \qquad (4.2)$$

where,

$\bar{\sigma}$ = effective normal stress

$\bar{c}$ = true cohesion

$\bar{\phi}$ = true angle of friction.

However,

$$\bar{\sigma} = \sigma - u \qquad (4.3)$$

where,

u = pore water pressure

and equation 4.2 can be expressed as:

$$s = \bar{c} + (\sigma - u)\tan\bar{\phi} \qquad (4.4)$$

All the triaxial shear strength tests in this investigation were performed as unconsolidated-undrained (UU or Quick). These tests are performed so rapidly that no pore water can escape from the sample during testing. This testing procedure was considered to be simulating the most critical field conditions in that the traffic loads expected on this pavement are instantaneous and cyclic and do not allow draining of water from the shale matrix.

The samples were tested in the Clockhouse triaxial testing machine with the set-up shown in Figure 4.3. The loading capacity of the machine is 10,000 lbs and it is capable of applying deformation at the rate 0f 0.0007 in/min to 0.16 in/min. The liquid use in the pressure cell is a 75-25% mixture of distilled water and glycerine, respectively. The rate of shear deformation used was 0.05 in/min. All raw and stabilized shale samples were tested at the lateral pressures of 10 psi, 20 psi, and 30 psi. Typical sample failures are shown in Figure 4.4.

Direct Shear Test

The Direct Shear Test is a simple straightforward test to perform and is made by placing a shale sample into the shear box illustrated in Figure 4.5. The box is

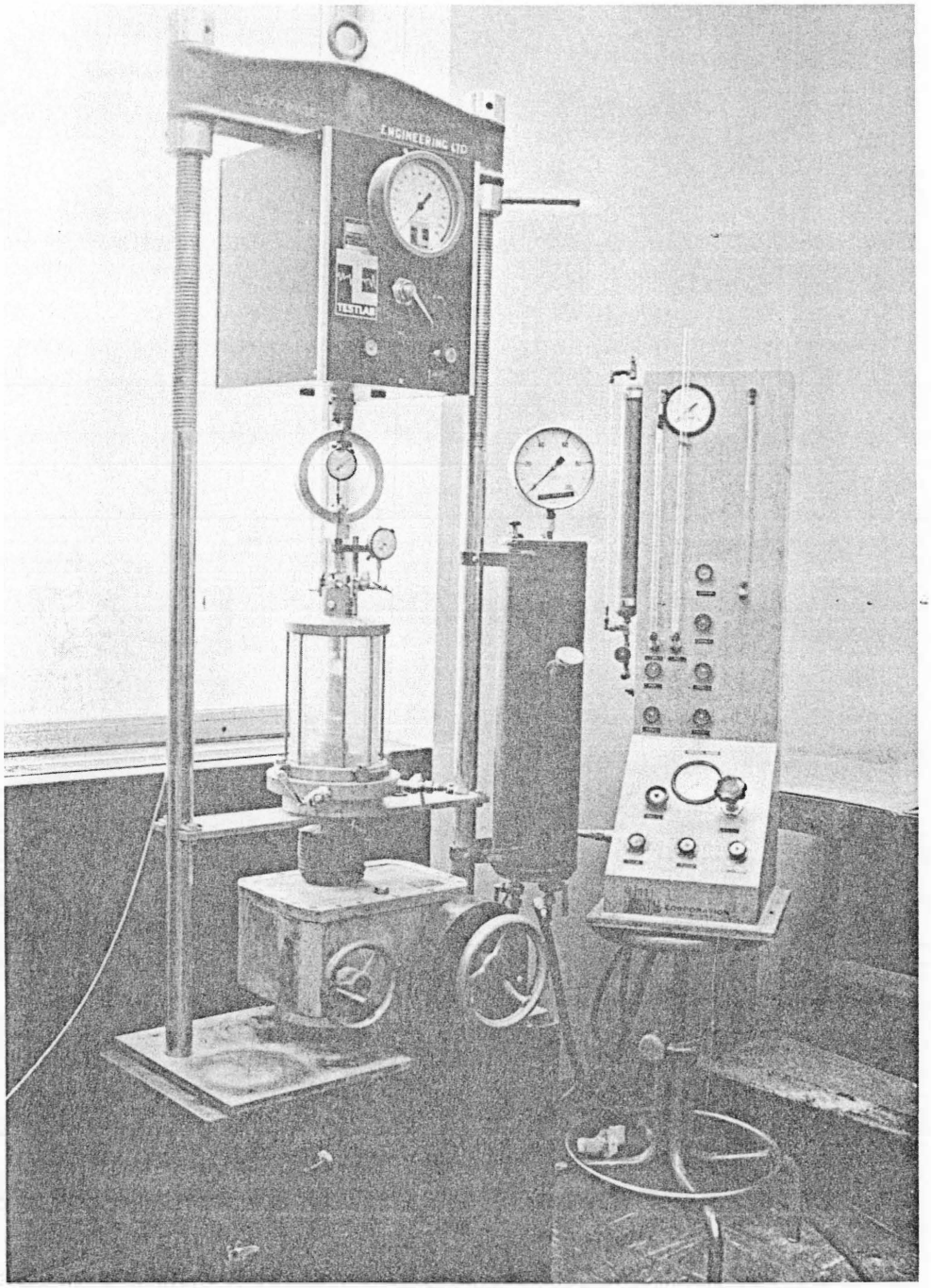

Figure 4.3 Triaxial compression test set up.

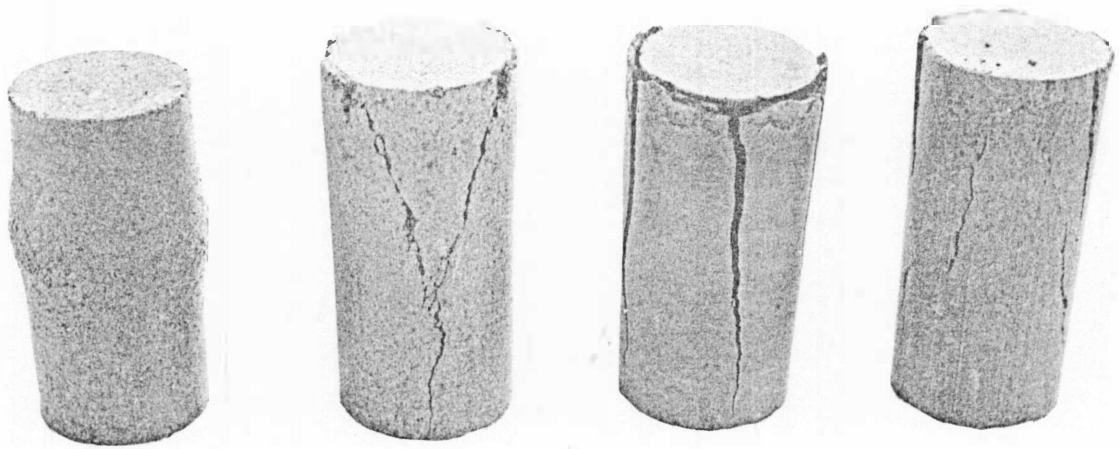

(a) (b) (c) (d)

Figure 4.4 Failure patterns of triaxial samples.

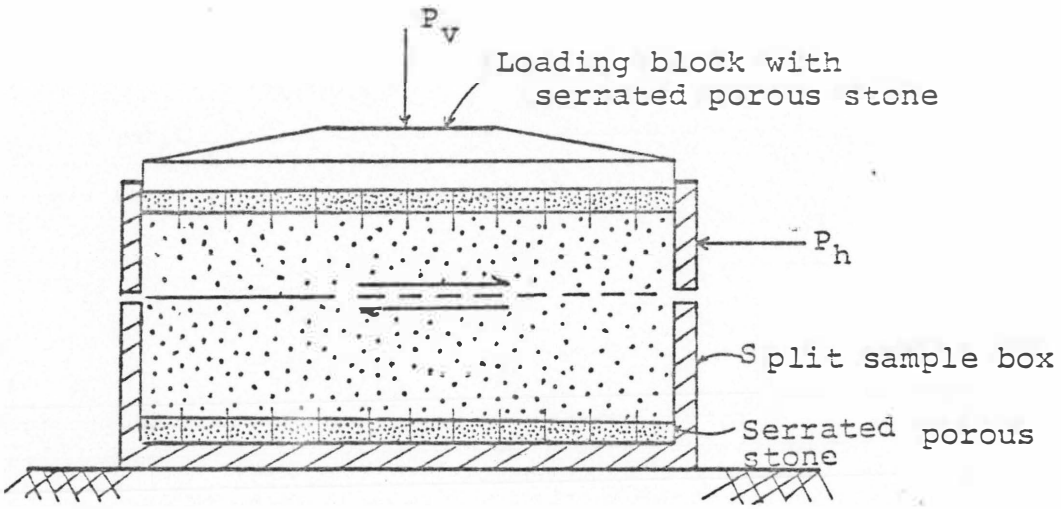

Figure 4.5 Direct shear schematic.

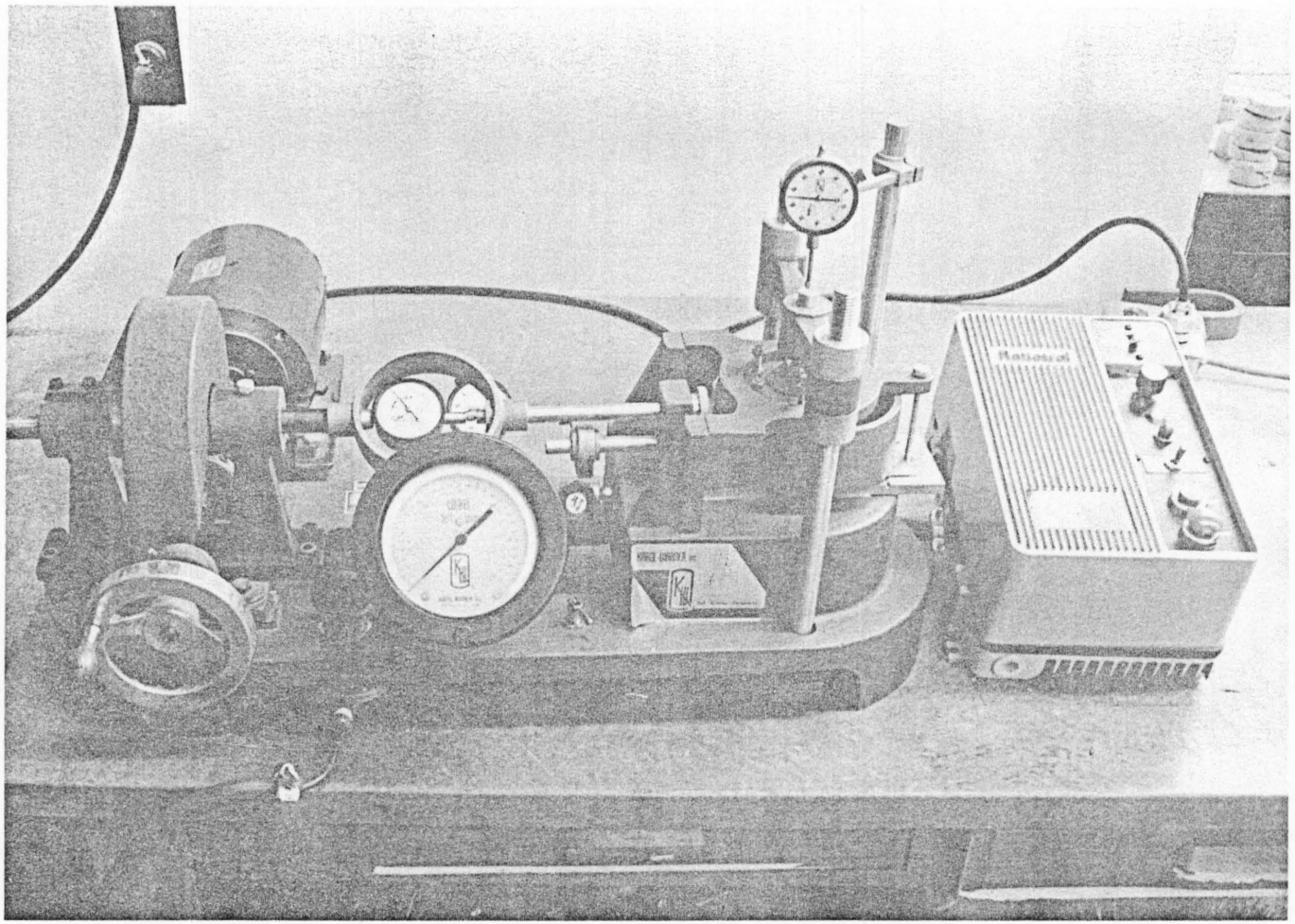

Figure 4.6 Direct shear test set up.

correspond to 1,000 psf, 4,000 psf, and 8,000 psf, respectively. The samples failed in approximately the same pattern as shown in Figure 4.7.

(a) (b) (c) (d)

Figure 4.7 Failure patterns of direct shear samples.

CHAPTER V

PRESENTATION AND DISCUSSION OF DATA

The main scope of this study was to determine the strength characteristics of stabilized shale samples on the basis of unconsolidated-undrained triaxial shear test and direct shear tests. An attempt was also made to correlate the results of the two tests and to evaluate the values of cohesion, c, and the angle of internal friction, ϕ, calculated from the two tests. A comparison is also made with respect to the above mentioned parameters, between dry samples and samples immersed in water for 12 hours. All samples were cured for 28 days at 90-100% relative humidity and at two temperatures: one set at 70°F and the other at 110°F.

Grain Size Analysis

The grain size distribution curves for raw and ultrasonically treated shale are presented in Figure 5.1 and the textural composition in Table 5.1.

Moisture Density Relationships

The first step in any research on the effects of stabilization of soils is to determine the relationships of

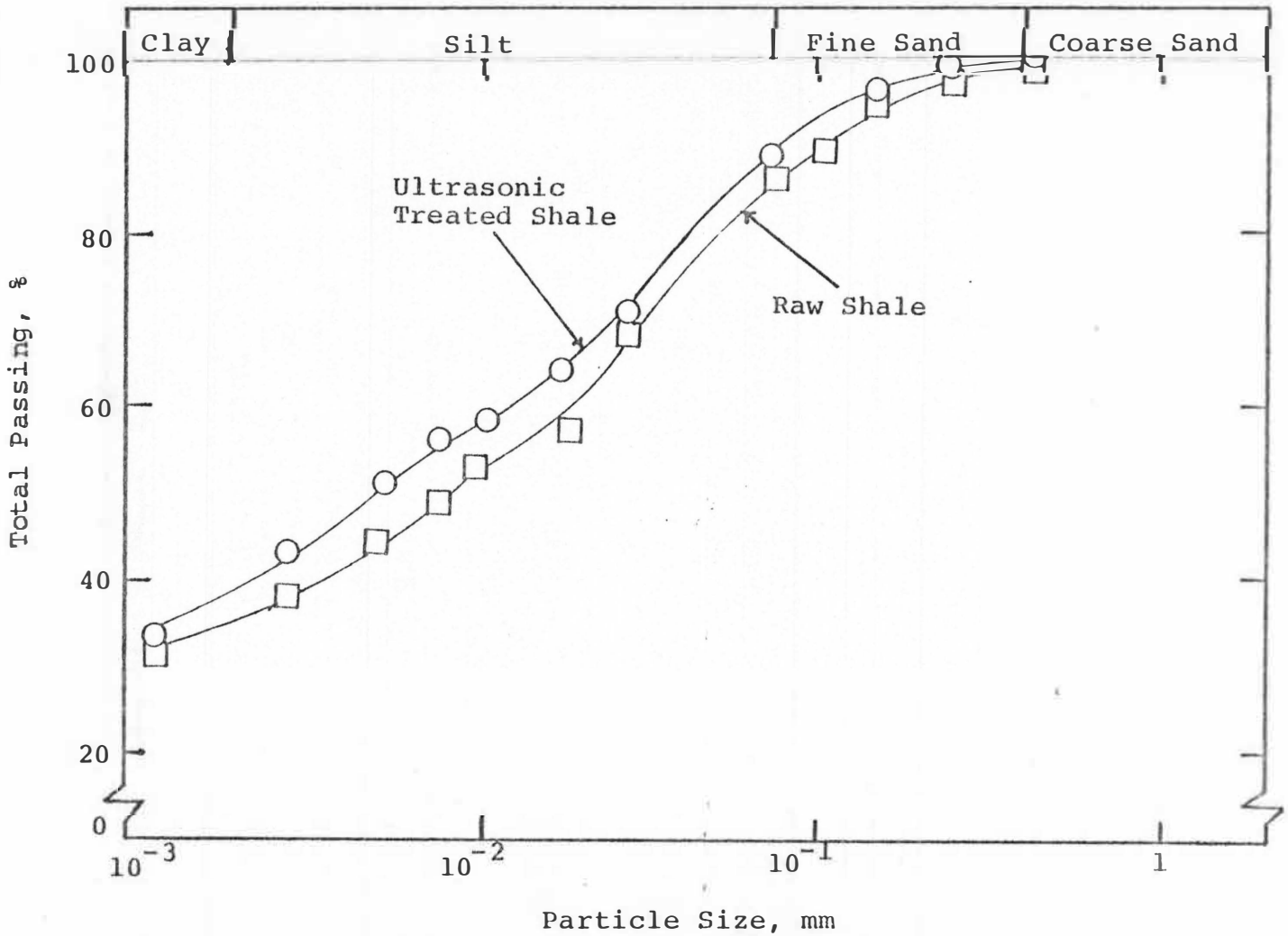

Figure 5.1 Grain size distribution curve.

TABLE 5.1

GRAIN SIZE ANALYSIS OF SHALE

Condition	<2μ-clay %	Silt %	Fine sand %
Raw shale	35	51	12
After ultra-sonic treatment	39	47	11

maximum dry density and optimum moisture content with the amount of stabilizing agents added to the soil. The results of these relationships are presented in Table 4.1.

In comparing the density moisture properties of raw shale and the corresponding stabilized forms, the following observations can be made. Addition of flyash increased the maximum dry density from 113.2 pcf to 116.2 pcf, while optimum moisture content remained the same as that of the raw shale. Lime treatment caused a decrease in maximum dry density from 113.2 pcf to 106.8 pcf, while the optimum moisture content was increased from 14.2% to 19.0%. This confirms the findings of other investigators (Kumar, 1974). Addition of portland cement decreased slightly the maximum dry density (MDD) from 113.2 pcf to 110.0 pcf and the optimum moisture content (OMC) was increased from 14.2% to 16.0%.

The observed decreases in MDD and increases in OMC of the cement and lime stabilized shale are attributed to flocculation and aggregation of clay particles caused by ion exchange between them and lime, and cement particles. The Federal Highway Administration (1978), reports that flocculation of shale-clays could also be attributed to a reduction in sliding friction implemented through modification of electrical double-layer interactions.

Atterberg Limits

The liquid limit and plasticity index values are presented in Table 5.2. The plastic limit for the raw shale was found to be 11%. Lime and flyash stabilization increased the plastic limit to 22% and 24%, respectively. Lime stabilization reduced the liquid limit to 32% while flyash stabilization caused an even lower reduction to 29%. The plasticity index of the portland cement treated shale was found to be zero while the plastic limit could not be determined. Generally, the addition of lime, portland cement, and flyash reduced the plasticity index of the shale considerably.

The graphical representation of the plasticity index of raw shale and shale additive mixtures is presented in Figure 5.3 in the form of block diagram.

Triaxial Strength Test Results

During the ejection of triaxial samples, using the extraction plunger, it was observed that densification was slightly increased at the ends of all samples. It may be stated that the ejection process has caused some increase in density.

The sample identifications were made according to the sequence shown in Table 5.3.

Failure Loads

In the triaxial shear test, failure was considered at a stress beyond which the actual vertical stress started

TABLE 5.2

PLASTIC PROPERTIES OF RAW AND STABILIZED SHALE

Type of Shale	70°F			110°F		
	Plastic limit (%)	Liquid limit (%)	Plasticity index (%)	Plastic limit (%)	Liquid limit (%)	Plasticity index (%)
RAW	11	36	25	10	37	27
SHALE+L	22	32	10	21	31	10
SHALE+PC	NP	33	NP	NP	31	0
SHALE+FA	24	29	5	28	31	3

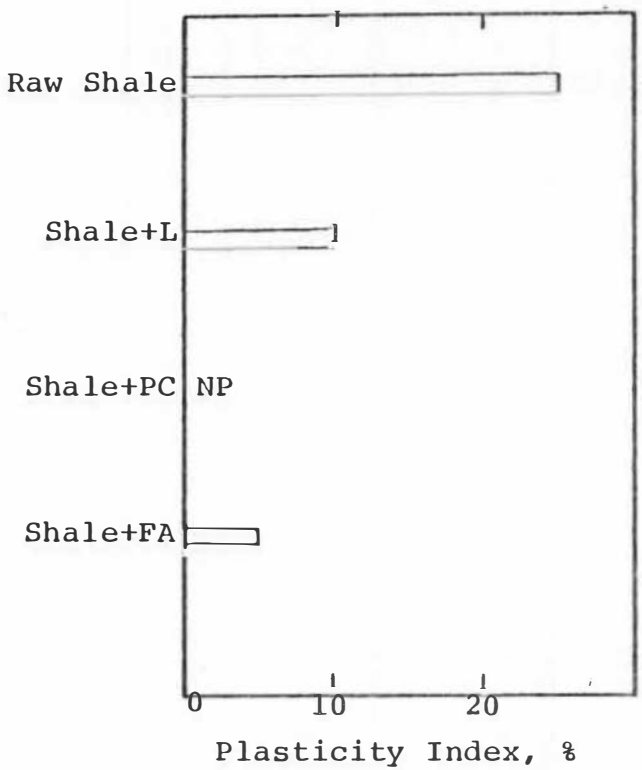

Figure 5.2 Plasticity index of raw and stabilized shale.

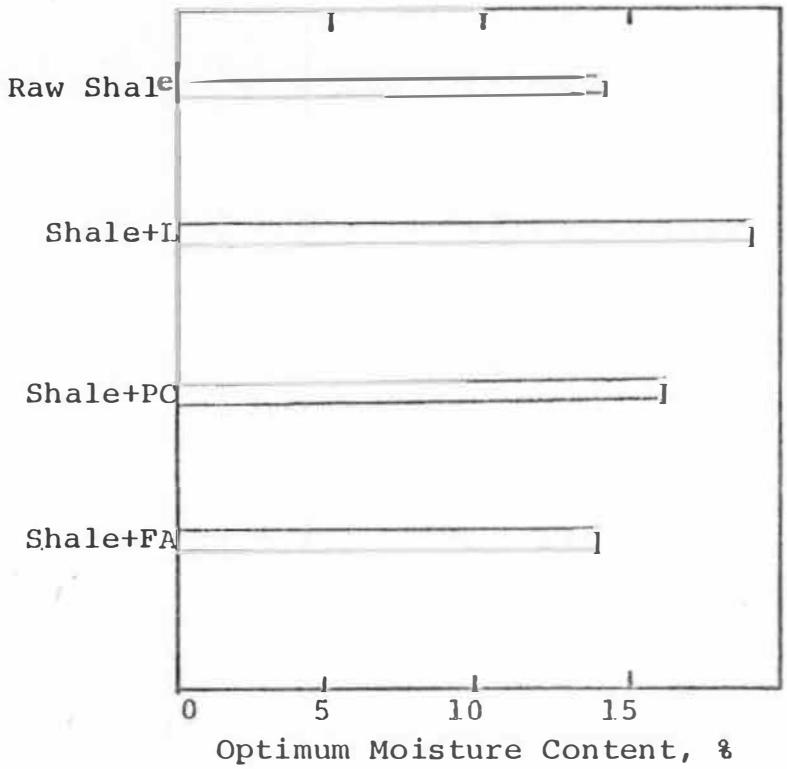

Figure 5.3 Optimum moisture content of raw and stabilized shale.

TABLE 5.3

SYMBOL EXPLANATION

Notation	Explanation	Graphical Symbol
L-70-0	Shale + 5% Lime, cured at 70°F, 0-hr delayed compaction	dry O, wet ●
L-110-2	Shale + 5% Lime, cured at 110°F, 2-hrs delayed compaction	dry O, wet ●
PC-70-0	Shale + 12% Cement, cured at 70°F, 0-hr delayed compaction	dry □, wet ■
PC-110-2	Shale + 12% Cement, cured at 110°F, 2-hr delayed compaction	dry □, wet ■
FA-70-0	Shale + 25% Flyash, cured at 70°F, 0-hr delayed compaction	dry ▽, wet ▼
FA-110-2	Shale + 25% Flyash, cured at 110°F, 2-hr delayed compaction	dry ▽, wet ▼

to decrease. The Mohr-Coulomb equation discussed in Chapter IV, which is used to determine the cohesion, c, and the angle of internal friction, ϕ, by means of lines drawn tangentially to the Mohr circles, was not employed in this study. The stress path method, which indicates the way the vertical stress impacts on the strength in conjuction with the lateral stress, was found to be perhaps more meaningful. In employing this method the two parameters are calculated. These are p and q and are given by:

$$p = (\sigma_1 + \sigma_3)/2 \qquad (5.1)$$

$$q = (\sigma_1 - \sigma_3)/2 \qquad (5.2)$$

where,

σ_1 = major principal stress

σ_3 = minor principal stress

The failure envelopes obtained from the p-q diagrams are referred to as K_f-lines or modified Mohr-Coulomb failure envelopes.

The shear strength parameters c and ϕ are calculated from the intercept, a, and the slope ($\tan\alpha$) of the modified Mohr-Coulomb failure envelope, an example of which is shown in Figure 5.4, using the following expressions:

$$\phi = \sin^{-1}(\tan\alpha) \qquad (5.3)$$

$$c = a/(\cos\phi) \qquad (5.4)$$

This approach of stress path was found to be superior to the conventional method due to the fact that σ_3 values were small and σ_1 high, thus, presenting difficulties in plotting

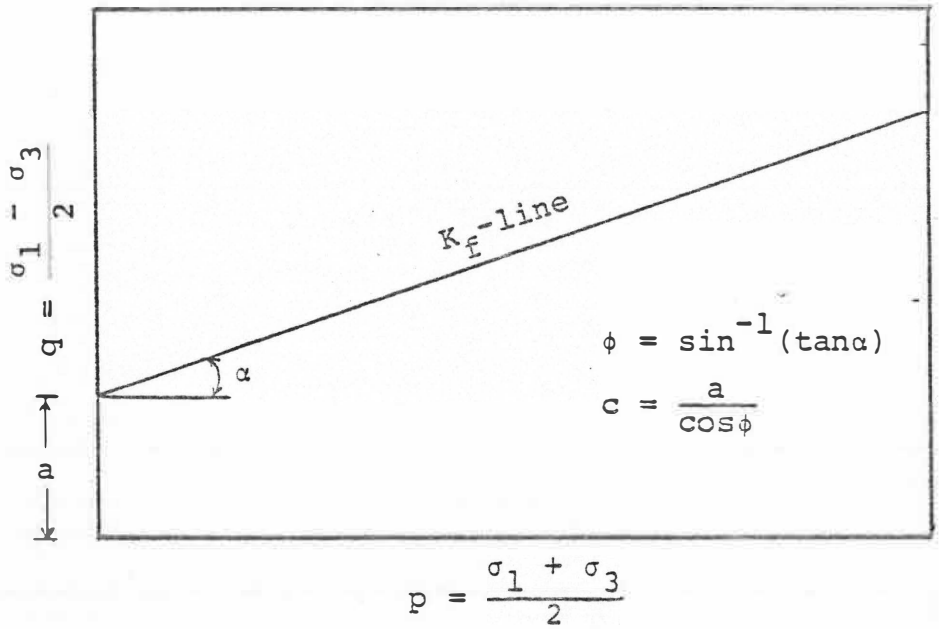

Figure 5.4 Illustrative p-q diagram.

the Mohr circles. Values of failure loads obtained from triaxial tests results of raw shale and lime, portland cement, and flyash stabilized shale are presented in Table 5.4 for samples cured at 70°F and in Table 5.5 for samples cured at 110°F. Strength values obtained from samples immersed in water for 12 hrs and those obtained from samples compacted after a 2-hr delay are also included in Tables 5.4 and 5.5. All p-q diagrams are presented in Appendix A.

Dry and Immersed Strengths

Failure loads for samples immersed in water for 12 hrs are less than their dry counterparts in all cases. Triaxial shear strengths of raw samples cured for 28 days at temperatures of 70°F and 110°F and 100% relative humidity were high when tested dry. This is attributed to the very small radii of the meniscus which has the tendency to pull the particles together.

Effect of Temperature

Failure loads of raw and stabilized shale samples were found to be considerably higher for the samples cured at 110°F and 100% relative humidity, compared to those cured at 70°F and 100% relative humidity. This confirms earlier findings of other investigators (Jha, 1977). Shale samples stabilized with portland cement appear to have been more affected by the temperature increase than the lime and flyash stabilized samples. Raw samples cured at 70°F and

TABLE 5.4

FAILURE STRESS (PSI) FROM TRIAXIAL TEST
OF RAW AND STABILIZED SHALE

Type of Shale	Lateral Pressure (psi)	Compaction and Testing Condition			
		Dry		Immersed	
		0-hr	2-hr	0-hr	2-hr
R-70	10	1025.0	726.0	ND*	ND*
	20	1069.0	769.0	ND*	ND*
	30	1014.0	931.0	ND*	ND*
L-70	10	937.0	1017.0	901.0	1083.0
	20	978.0	1083.0	950.0	939.0
	30	1041.0	1167.0	951.0	978.0
PC-70	10	1645.0	1512.0	1546.0	1520.0
	20	1773.0	1654.0	1577.0	1599.0
	30	1993.0	1735.0	1745.0	1717.0
FA-70	10	1183.0	1150.0	1125.0	1005.0
	20	1332.0	1285.0	1142.0	1065.0
	30	1353.0	1337.0	1175.0	1109.0

ND* cannot be determined due to disintegration following the first hour of immersion.

TABLE 5.5

FAILURE STRESS (PSI) FROM TRIAXIAL TEST
OF RAW AND STABILIZED SHALE

Type of Shale	Lateral Pressure (psi)	Compaction and Testing Condition			
		Dry		Immersed	
		0-hr	2-hr	0-hr	2-hr
R-110	10	1058.0	861.0	ND*	ND*
	20	960.0	1001.0	ND*	ND*
	30	965.0	1090.0	ND*	ND*
L-110	10	1512.0	1017.0	1266.0	946.0
	20	1262.0	1083.0	1430.0	978.0
	30	1569.0	1167.0	1369.0	1024.0
PC-110	10	2050.0	1819.0	1878.0	1648.0
	20	2163.0	1954.0	1961.0	1688.0
	30	2151.0	2184.0	2043.0	2006.0
FA-110	10	1380.0	1586.0	1085.0	1238.0
	20	1665.0	1491.0	1183.0	1305.0
	30	1366.0	1577.0	1326.0	1114.0

ND* cannot be determined due to disintegration following the first hour of immersion.

110°F disintegrated during the first hour of immersion; therefore, no testing was possible.

Delayed Compaction

The effect of a 2-hr delayed compaction on the strength characteristics was evaluated on raw and stabilized shales. Triaxial shear strengths were determined for dry as well as immersed samples cured at 70°F and 110°F. The results are presented in Tables 5.4 and 5.5. For raw shale, portland cement and flyash stabilized shale delayed compaction of 2 hours, showed a tendency to decrease the failure loads.

The lime stabilized shale, however, remained an exception and it manifested an increase in the failure loads after delayed compaction.

Cohesion

The values of cohesion, c, of the raw and stabilized shale cured at 70°F and 110°F are given in Tables 5.6 and 5.7, respectively. In general, stabilization caused an increase in the cohesion due to the flocculation and bonding of the shale particles.

Lime stabilization. The cohesion of shale stabilized with lime and cured at 70°F but no delay in compaction shows an increase from 137.0 psi to 147.0 psi. Under a 2-hr delayed compaction condition, the cohesion increased from 104.0 psi to 173.0 psi. The 12-hr immersion in water

TABLE 5.6

COHESION (PSI) FROM TRIAXIAL TEST
OF RAW AND STABILIZED SHALE

Type of Shale	Compaction and Testing Condition			
	Dry		Immersed	
	0-hr	2-hr	0-hr	2-hr
R-70	137.0	104.0	ND*	ND*
L-70	147.0	173.0	161.0	188.0
PC-70	205.0	163.0	217.0	218.0
FA-70	167.0	122.0	208.0	153.0

ND* cannot be determined due to disintegration following the first hour of immersion.

TABLE 5.7

COHESION (PSI) FROM TRIAXIAL TEST
OF RAW AND STABILIZED SHALE

Type of Shale	Compaction and Testing Condition			
	Dry		Immersed	
	0-hr	2-hr	0-hr	2-hr
R-110	72.0	83.0	ND*	ND*
L-110	160.0	185.0	157.0	156.0
PC-110	122.0	218.0	153.0	162.0
FA-110	154.0	126.0	138.0	84.0

ND* cannot be determined due to disintegration following the first hour of immersion.

gave a cohesion of 161.0 psi while the raw samples disintegrated. The cohesion of samples cured at 110°F but no delay in compaction increased from 72.0 psi to 160.0 psi.

Cement stabilization. Cement stabilization resulted in a considerable increase in the cohesion. Stabilized samples cured at 70°F but no delay in compaction attained a cohesion of 205.0 psi, while raw samples tested under similar conditions had a cohesion of 137.0 psi. Generally, cement stabilization produced a higher value of cohesion than lime or flyash stabilization.

Flyash stabilization. The cohesion values of stabilized shale are higher than those of the raw shale. Flyash stabilized samples cured at 70°F and tested in the dry conditions but no delay in compaction, produced a cohesion of 167.0 psi. Delay in compaction reduced the value of cohesion to 122.0 psi.

Angle of Internal Friction

The values of the internal friction, ϕ, of raw and stabilized shales cured at 70°F and 110°F are depicted in Tables 5.8 and 5.9, respectively. The angle of internal friction of samples cured at 70°F decreased as a result of stabilization. Samples cured at 110°F produced a higher angle of internal friction than samples cured at 70°F. A general trend, however, is difficult to be detected.

TABLE 5.8

ANGLE OF INTERNAL FRICTION (DEGREES) FROM TRIAXIAL TEST OF RAW AND STABILIZED SHALE

Type of Shale	Compaction and Testing Condition			
	Dry		Immersed	
	0-hr	2-hr	0-hr	2-hr
R-70	59	58	ND*	ND*
L-70	57	53	43	43
PC-70	54	53	53	64
FA-70	53	60	48	38

ND* cannot be determined due to disintegration following the first hour of immersion.

TABLE 5.9

ANGLE OF INTERNAL FRICTION (DEGREES) FROM TRIAXIAL TEST OF RAW AND STABILIZED SHALE

Type of Shale	Compaction and Testing Condition			
	Dry		Immersed	
	0-hr	2-hr	0-hr	2-hr
R-110	62	61	ND*	ND*
L-110	51	45	55	44
PC-110	60	68	67	60
FA-110	72	62	64	62

ND* cannot be determined due to disintegration following the first hour of immersion.

Lime stabilization. Lime stabilized samples cured at 70°F but no delay in compaction displayed no significant change in the value of the angle of internal friction, ϕ. On the other hand, delayed compaction decreased ϕ from 59° to 53°. Immersion in water caused a further decrease in ϕ to 43°. Samples cured at 110°F but no delay in compaction attained a value of ϕ of 51° while their counterparts cured at 70°F showed ϕ to be 57°.

Cement stabilization. The angle of internal friction, ϕ, of portland cement stabilized samples cured at 70°F but no delay in compaction and tested in the dry condition, was found to be 54°. Samples cured at 110°F and tested under similar conditions, gave an angle of internal friction of 60°. Delay in compaction decreased ϕ from 67° to 60° for samples tested in the immersed condition.

Flvash stabilization. Flyash stabilized samples cured at 70°F and tested after emmersion displayed a significant decrease in the angle of internal friction. Likewise, delay in compaction decreased the value of ϕ in all cases. For example, samples cured at 110°F but no delay in compaction showed the value of ϕ to be 72° while for samples compacted after a 2-hr delay the value of ϕ decreased to 62°.

Direct Shear Test Results

Failure Loads

In all direct shear tests, failure was considered to have occurred at a stress beyond which the actual lateral stress started to decrease. The plot of the normal stress versus shear stress is commonly used to determine the strength parameters c and ϕ. An illustration of such a graph is shown in Figure 5.5. As shown in Figure 5.5 the intercept is the cohesion c, and the slope of the failure envelope is the angle of internal friction ϕ.

Values of shear stress at failure are presented in Tables 5.10 and 5.11 for samples cured at 70°F and 110°F, respectively. Graphical representations of lateral stress versus vertical stress are presented in Appendix B.

Dry and Immersed Strengths

It was observed that samples immersed in water failed at shear stresses slightly less than their dry counterparts. As the vertical loads increased, the shearing failure stress also increased. Values of dry and immersed strengths of samples cured at 70°F are presented in Table 5.10 and for samples cured at 110°F in Table 5.11.

Effect of Temperature

Stabilized samples cured at 110°F failed at shear stresses higher than the failure stresses of samples cured at 70°F. Shale stabilized with portland cement appeared to

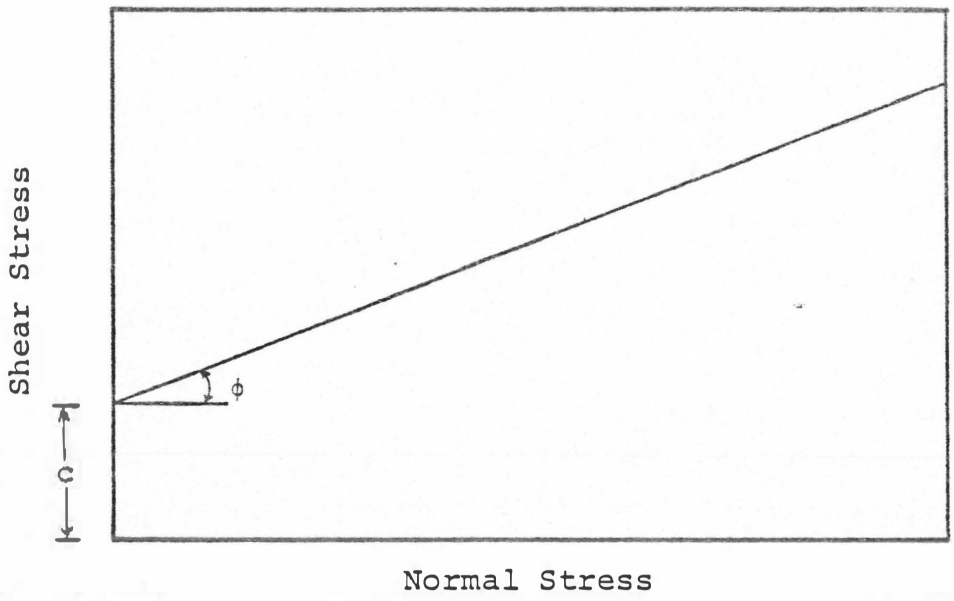

Figure 5.5 Typical plot of direct shear test on cohesive soil.

TABLE 5.10

FAILURE STRESS (PSI) FROM DIRECT SHEAR TEST OF RAW AND STABILIZED SHALE

Type of Shale	Vertical Stress (psi)	Compaction and Testing Condition			
		Dry		Immersed	
		0-hr	2-hr	0-hr	2-hr
R-70	7	3.20	3.30	ND*	ND*
	28	4.80	4.30	ND*	ND*
	56	3.00	5.80	ND*	ND*
L-70	7	4.81	5.20	4.10	4.25
	28	7.00	5.26	5.10	3.84
	56	10.00	8.70	7.70	8.14
PC-70	7	24.20	21.60	16.62	13.30
	28	26.50	22.00	16.43	18.50
	56	30.80	22.00	26.70	20.70
FA-70	7	4.87	7.26	5.97	2.32
	28	10.90	9.58	8.32	7.32
	56	17.75	13.75	9.32	9.26

ND* cannot be determined due to disintegration following the first hour of immersion.

TABLE 5.11

FAILURE STRESS (PSI) FROM DIRECT SHEAR TEST OF RAW AND STABILIZED SHALE

Type of Shale	Vertical Stress (psi)	Compaction and Testing Condition			
		Dry		Immersed	
		0-hr	2-hr	0-hr	2-hr
R-110	7	3.84	4.68	ND*	ND*
	28	4.58	5.48	ND*	ND*
	56	5.35	6.68	ND*	ND*
L-110	7	15.17	10.65	12.62	9.62
	28	19.14	11.94	16.71	11.94
	56	18.62	17.75	21.96	16.90
PC-110	7	30.91	21.72	25.66	12.42
	28	ND**	23.37	ND**	19.04
	56	ND**	22.00	ND**	19.84
FA-110	7	16.45	6.36	6.07	4.20
	28	15.65	11.10	6.67	7.35
	56	20.50	12.94	9.55	9.65

ND* cannot be determined due to disintegration following the first hour of immersion.
ND** loading was discontinued and samples did not break.

be more affected by the temperature increase than the lime and flyash stabilized shale. Raw samples disintegrated during the first hour of immersion, therefore no testing was possible.

Delayed Compaction

A study of two-hours delayed compaction was conducted on raw and stabilized samples. Direct shear strengths were determined for dry as well as immersed samples cured for 28 days at 70°F and 110°F and 100% relative humidity. The results are presented in Tables 5.10 and 5.11. For all samples, raw and stabilized, the 2-hr delay has caused a slight decrease in the shear strength.

Cohesion

The data on cohesion, c, of raw and stabilized shale are presented in Table 5.12 for samples cured at 70°F and Table 5.13 for samples cured at 110°F. The cohesion of all stabilized samples was found to be higher than the cohesion of raw samples. All stabilized samples immersed in water for 12-hrs have shown some cohesive strength as opposed to their raw counterparts which disintegrated during the first hour of immersion.

Lime stabilization. As a result of lime stabilization the cohesion of the raw shale increased from 3.0 psi to 4.0 psi for dry samples cured at 70°F. Lime stabilized samples cured at 110°F showed a cohesion of 12.0 psi when

TABLE 5.12

COHESION (PSI) FROM DIRECT SHEAR TEST
OF RAW AND STABILIZED SHALE

Type of Shale	Compaction and Testing Condition			
	Dry		Immersed	
	0-hr	2-hr	0-hr	2-hr
R-70	3.00	3.00	ND*	ND*
L-70	4.00	3.50	2.00	2.00
PC-70	22.00	21.00	14.00	12.00
FA-70	4.00	6.00	5.00	4.00

ND* cannot be determined due to disintegration following the first hour of immersion.

TABLE 5.13

COHESION (PSI) FROM DIRECT SHEAR TEST
OF RAW AND STABILIZED SHALE

Type of Shale	Compaction and Testing Condition			
	Dry		Immersed	
	0-hr	2-hr	0-hr	2-hr
R-110	4.00	4.00	ND*	ND*
L-110	12.10	8.00	11.00	6.00
PC-110	ND**	21.00	ND**	12.00
FA-110	10.00	6.00	5.00	4.00

ND* cannot be determined due to disintegration following the first hour of immersion.
ND** loading was discontinued and samples did not break.

tested dry as opposed to their raw counterparts which attained a cohesive strength of 4.0 psi.

Cement stabilization. Cement stabilization contributed to the highest gain in cohesive strength. The cohesion of cement stabilized shale cured at 70°F but no delay in compaction was 22.0 psi, which far exceeds that of lime and flyash stabilized samples. Cement stabilized samples cured at 110°F and tested dry, attained a cohesive strength of 35.0 psi without any indication of up-coming failure. At this point, however, loading was discontinued to avoid permanent deformation of the proving ring which is not capable of carrying higher loads. The 2-hr delay compaction decreased the cohesive strength of the stabilized shale as did immersion in water.

Flyash stabilization. The cohesive strength of flyash stabilized shale increased from 3.0 psi to 4.0 psi for samples cured at 70°F but no delay in compaction. Immersion in water did not cause any significant decrease or increase in cohesion. Samples cured at 110°F and tested dry with no delay in compaction gave an increase in cohesion from 4.0 psi to 10.0 psi. Delay in compaction decreased the cohesion to 6.0 psi for samples tested under the same conditions. Immersion in water also decreased the cohesion to 5.0 psi.

Angle of Internal Friction

The values of the angle of internal friction of raw and stabilized shales are presented in Tables 5.14 and 5.15 for samples cured at 70°F and 110°F, respectively. The general trend is that stabilization increased the angle of internal friction.

Lime stabilization. Lime stabilized samples cured at 70°F gave higher cohesion than the raw shale. Under immediate compaction and 110°F curing temperature stabilization changed the angle of internal friction from 3° to 15°. Delay in compaction has caused a slight decrease in the value of the internal friction angle. Immersion, on the other hand, did not cause any significant changes in ϕ.

Cement stabilization. Cement stabilized samples compacted without delay displayed a slight increase in ϕ from 8.5° to 10°. On the other hand, delayed compaction caused a decrease in the value of ϕ. For example, cement stabilized shale, cured at 70°F but no delay in compaction showed ϕ to be 10° while the 2-hr delay in compaction gave the value of 3° for ϕ. For cement stabilized samples cured at 110°F but no delay in compaction the angle of internal friction was not measured because loading was discontinued and the samples were not allowed to break.

Flyash stabilization. Flyash stabilized samples cured at 70°F but no delay in compaction displayed an increase in the angle of internal friction from 8.5° to 16°.

TABLE 5.14

ANGLE OF INTERNAL FRICTION (DEGREES) FROM DIRECT SHEAR TEST OF RAW AND STABILIZED SHALE

Type of Shale	Compaction and Testing Condition			
	Dry		Immersed	
	0-hr	2-hr	0-hr	2-hr
R-70	8.5	4	ND*	ND*
L-70	8	6	6	8
PC-70	10	3	11	11
FA-70	16	9	10	8

ND* cannot be determined due to disintegration following the first hour of immersion.

TABLE 5.15

ANGLE OF INTERNAL FRICTION (DEGREES) FROM DIRECT SHEAR TEST OF RAW AND STABILIZED SHALE

Type of Shale	Compaction and Testing Condition			
	Dry		Immersed	
	0-hr	2-hr	0-hr	2-hr
R-110	3	3	ND*	ND*
L-110	15	8	13	9
PC-110	ND**	7	ND**	10
FA-110	12	9	7	8

ND* cannot be determined due to disintegration following the first hour of immersion.
ND** loading was discontinued and samples did not break.

Delay in compaction decreased the value of ϕ from 16^{o} to 9^{o}. Immersion in water also decreased the value of ϕ.

Discussion of Triaxial and Direct Shear Test Results

Failure loads obtained from triaxial shear tests were found to be slightly higher than those reported by Jha (1977) on a similar shale. Direct shear test results showed values for cohesion and angle of internal friction much lower than those obtained from triaxial tests. For example, flyash stabilized samples cured at $70^{o}F$ and without delay in compaction displayed a cohesion of 167.0 psi and an angle of internal friction of 53^{o}, while direct shear testing resulted in a cohesion of 4.0 psi and angle, ϕ, of 16^{o}. Lime and cement stabilized samples produced even greater differences in the two mentioned strength parameters. The data on cohesion, c, and angle of internal friction, ϕ, are plotted in Figures 5.6 to 5.9 where the subscripts TR and DR indicate values obtained from the triaxial test and direct shear test, respectively. These data suggest some relationships which cannot be mathematically expressed by a simple straight line. It is obvious that more data are necessary to make an evaluation based on sound statistical judgement. Nevertheless, a general trend appears to be in evidence. The triaxial test values both in c and ϕ are higher than the corresponding values obtained with the direct shear test. The distribution of these values does not lie along a straight line. Rather,

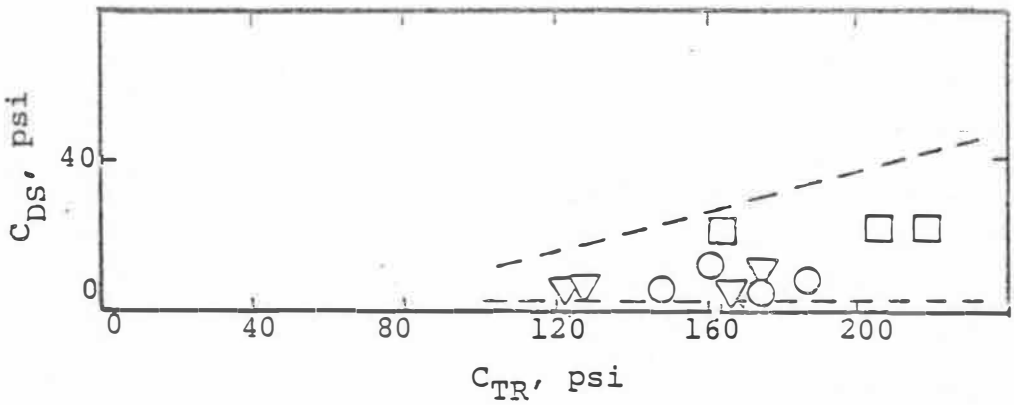

Figure 5.6 Cohesion values of dry stabilized samples cured for 28 days at 70°F and 100% relative humidity.

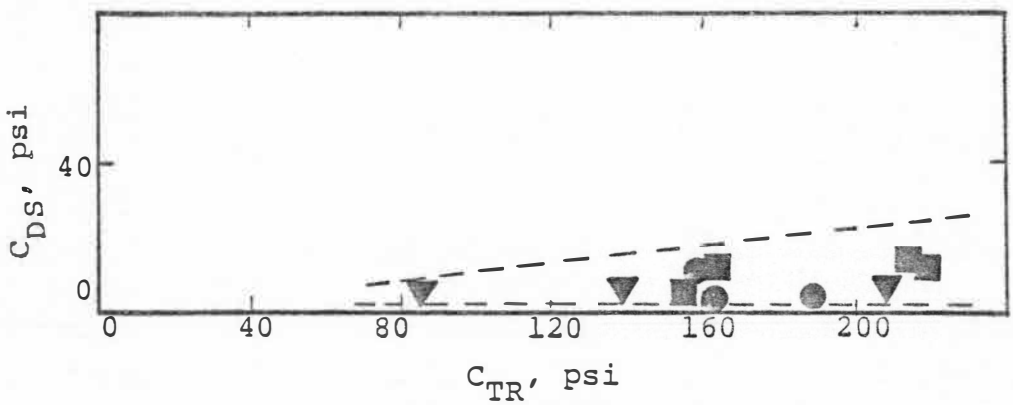

Figure 5.7 Cohesion values of wet stabilized samples cured for 28 days at 70°F and 100% relative humidity.

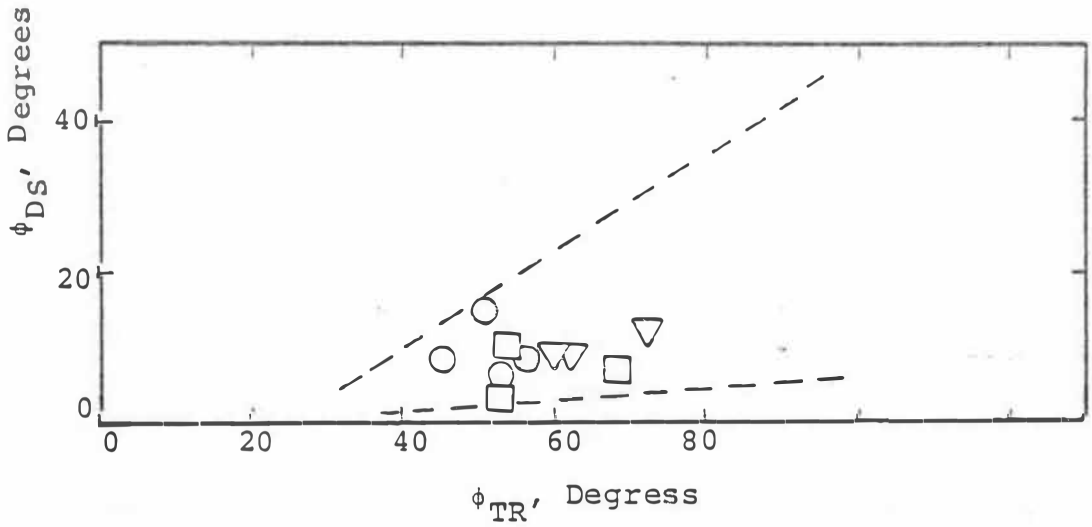

Figure 5.8 Cohesion values of dry stabilized samples cured for 28 days at 110°F and 100% relative humidity.

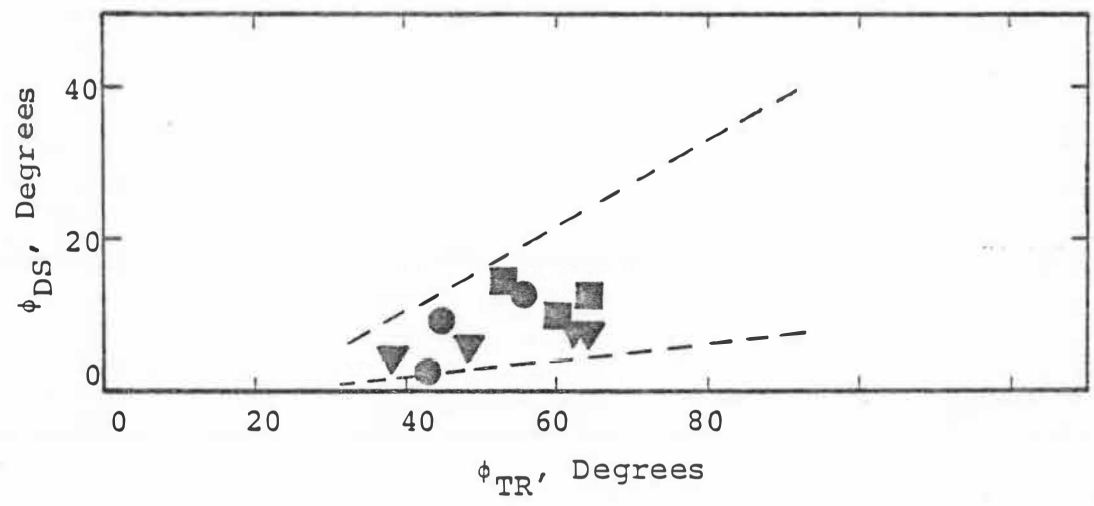

Figure 5.9 Cohesion values of wet stabilized samples cured for 28 days at 110°F and 100% relative humidity.

the values, as plotted in Figures 5.6 to 5.9, depict a fanning effect. As the c and ϕ values increase, the scatter increases.

Different factors may have contributed to such a variation of results. The method of compaction, for example, may be considered as a major contributing factor. The samples prepared for triaxial testing were compacted statically while the samples tested under direct shear were compacted dynamically. The plane of failure of the samples tested under direct shear is parallel to the plane of compaction. Any irregularities existing within the sample itself would be magnified when the sample is subjected to horizontal shearing stress. The cutting and trimming process employed to prepare the samples for direct shear testint may possibly and partly account for the observed variations.

The triaxial test has been widely used and has a history of reliable results. Therefore, to rely on the triaxial test results is plausible. Despite the fact that the results of this investigation are not conclusive enough to correlate the data obtained from the two testing procedures, the validity of the direct shear test must not be denied for samples compacted in the same manner and for undisturbed samples.

CHAPTER VI

CONCLUSIONS

The present laboratory investigation was conducted to evaluate the strength characteristics of lime, cement, and flyash stabilized samples and to examine the strength parameters c and ϕ. The data obtained provide the basis for arriving at the following principal conclusions:

1. Stabilization of the shale with the three additives has considerably increased the strength characteristics of the shale.
2. Cement stabilization imparted maximum dry and immersed strength gains but lime and flyash addition resulted in moderate but adequate strength gains.
3. Addition of lime, cement, and flyash to the shale, decreased considerably the plasticity index, as a result of clay particle cementation.
4. Cement stabilization and lime stabilization decrease the maximum dry density but increase the optimum moisture content.
5. Failure loads of all stabilized samples were reduced as a result of immersion in water.

6. The curing temperature of 110°F yields higher gain in strength compared to 70°F.
7. While, in the case of lime and cement stabilization, the angle of internal friction, ϕ, decreased, the increase in cohesion, c, was so high that it compensated for the decrease with the net result being an overall increase in the shear strength.
8. Partly due to the sample preparation procedure, the direct shear test results are not conclusive enough to be correlated with the triaxial test results.

CHAPTER VII

RECOMMENDATIONS

In view of the experience gained in this investigation, the following recommendations for future study appear to be in order:

1. To provide better design criteria, stabilized samples prepared in the laboratory, should be subjected to cyclic loading prior to triaxial testing.
2. Following the construction of the road, further testing should be done at different time intervals to evaluate the laboratory results.
3. Direct shear tests should be conducted on undisturbed samples obtained from the field prior to and after construction. Cyclic loading of the samples prior to testing should also be included.

REFERENCES

American Society of Civil Engineers, "Soil Improvement, History, Capabilities, and Outlook," New York, NY, 1978, pp. 52-53.

American Society for Testing Materials, "Terms Relating to Hydraulic Cement," Designation: C219-55, Book of Standards, Part 4, 1958

Bjerrum, L., "Geotechnical Properties of Norwegian Marine Clays," Geotechnique, Vol. 4, 1954a, pp. 49-50.

Bowles, Joseph E., "Foundation Analysis and Design," Second Edition, McGraw-Hill, 1977, pp. 29-30.

Bowles, Joseph E., "Physical and Geotechnical Properties of Soils," McGraw-Hill, 1979, pp. 353-354.

Davidson, D. T., and Handy, R.L., "Highway Engineering Handbook," McGraw-Hill, New York, N.Y., 1979, pp. 64-6.

Diamond, S., and Kinter, E. B., "Mechanics of Soil Lime Stabilization - An Interpretive Review," Public Roads, Vol. 33, No. 12, Bureau of Public Roads, U.S. Department of Commerce, Washington, D.C., 1966, pp. 260-265.

Diamond, S., White, J. L., and Dolch, W. L., "Transformation of Clay Minerals by Calcium Hydroxide Attack," 12th National Conference on Clay and Clay Minerals, Atlanta, Ga., 1963.

Goodman, Louis J., and Karol, R. H., "Theory and Practice of Foundation Engineering," McMillan Series in Civil Engineering, New York, N.Y., 1968, pp. 248-250.

Ingles, O. J., and Frydman, S., "The Effect of Cement and Lime on the Strength of Some Minerals and Its Relevance to the Stabilization of Australian Soils," Proceedings of the Stabilization of Australian Road Research Board Conference 2, 1966, pp. 1504-1528.

Jacabs, H. L., "Flyash Disposal," Sewage and Industrial Wastes, Vol. 22, Sept. 1950, pp. 1207-1213.

Jarrige, A., "Flyashes and Their Utilization," (Les Cendres Volantes et Leurs Possibites d'Utilsation) Annales des Mines (in French) Vol. 146, October and Novmeber 1957, pp. 649-672.

Jha, K., "Stabilization of Oklahoma Shales," A Ph.D. Dissertation, University of Oklahoma, Norman, Okla., 1977.

Kumar, S., "A Study of the Effects of Simulated Weathering and Repeated Loads on Four Lime Stabilized Oklahoma Shales," A Ph.D. Dissertation, University of Oklahoma, Norman, Okla., unpublished, 1974.

Laguros, J. G., "Effect of Chemicals on Soil-Cement Stabilization," A Ph.D. Dissertation, Iowa State University, Ames, Iowa, 1962.

Laguros, J. G., "Predictability of Physical Changes of Clay Forming Materials in Oklahoma," Report No. ODOH 68-03-2, OURI 1677, University of Oklahoma, School of Civil Engineering and Environmental Science, Norman, Okla., August 1972.

Laguros, J. G., and Jha, K., "Stabilization of Oklahoma Shales," Report No. ODOT 73-04-2, ORA 158-602, University of Oklahoma, School of Civil Engineering and Environmental Science, Norman, Okla., December 1977.

Moh, Z. C., "Reactions of Soil Minerals with Cement and Chemicals," Highway Research Board Record 56, 1965, pp. 39-61.

Morgan, R.E., "Utilization of Flyash," U.S. Department of the Interoir, Bureau of Mines, Information Circular 7635, June 1952.

National Lime Association, "Lime Stabilization of Roads," National Lime Association Bulletin No. 323, 1954.

Seed, H. B., Mitchell, J., and Chen, C. K., "Structure and Strength Characteristics of Compacted Clays," Journal of the Soil Mechanics and Foundation Division, Proc. of the ASCE, October 1960.

Skempton, A. W., and Henkel, D. J., "Tests on London Clay from Deep Borings at Paddington, Victoria, and South Bank," Proceedings of the 4th International Conference of Soil Mechanics Foundation Engineering, London, 1957, pp. 100-101.

Sloan, Richard L., "Early Reaction Determination in Two Hydroxide-Kaolinite System by Electron Microscopy and Diffraction, Clays and Clay Minerals," Proceedings of the 13th Conference, Pergamon Press, New York, N.Y., 1965, pp. 331-339.

Spangler, M. G., and Handy, Richard L., "Soil Engineering," International Textbook Company, Third Edition, New york, N.Y., 1973, pp. 428-429

Thompson, P. W., "Stack Dust Collection and Disposal," Power Plant Engineering, Vol. 51, October 1947, pp. 108-110.

Wang, Jerry W. H., "Role of Magnesium Oxide in Soil Lime Stabilization," Highway Research Board Special Report No. 90.

Weinheimer, C. M., "Flyash Disposal - A Mountaineous Problem," Electric Light and Power, Vol. 32, No. 5, April 1954, pp. 90-93.

Winterkorn, F. H., and Fang, H. Y., "Foundation Engineering HAndbook," Van Nostrand Reinolds Company, 1975, pp. 312-313

APPENDIX A

p-q DIAGRAMS OF DRY AND IMMERSED STABILIZED SAMPLES

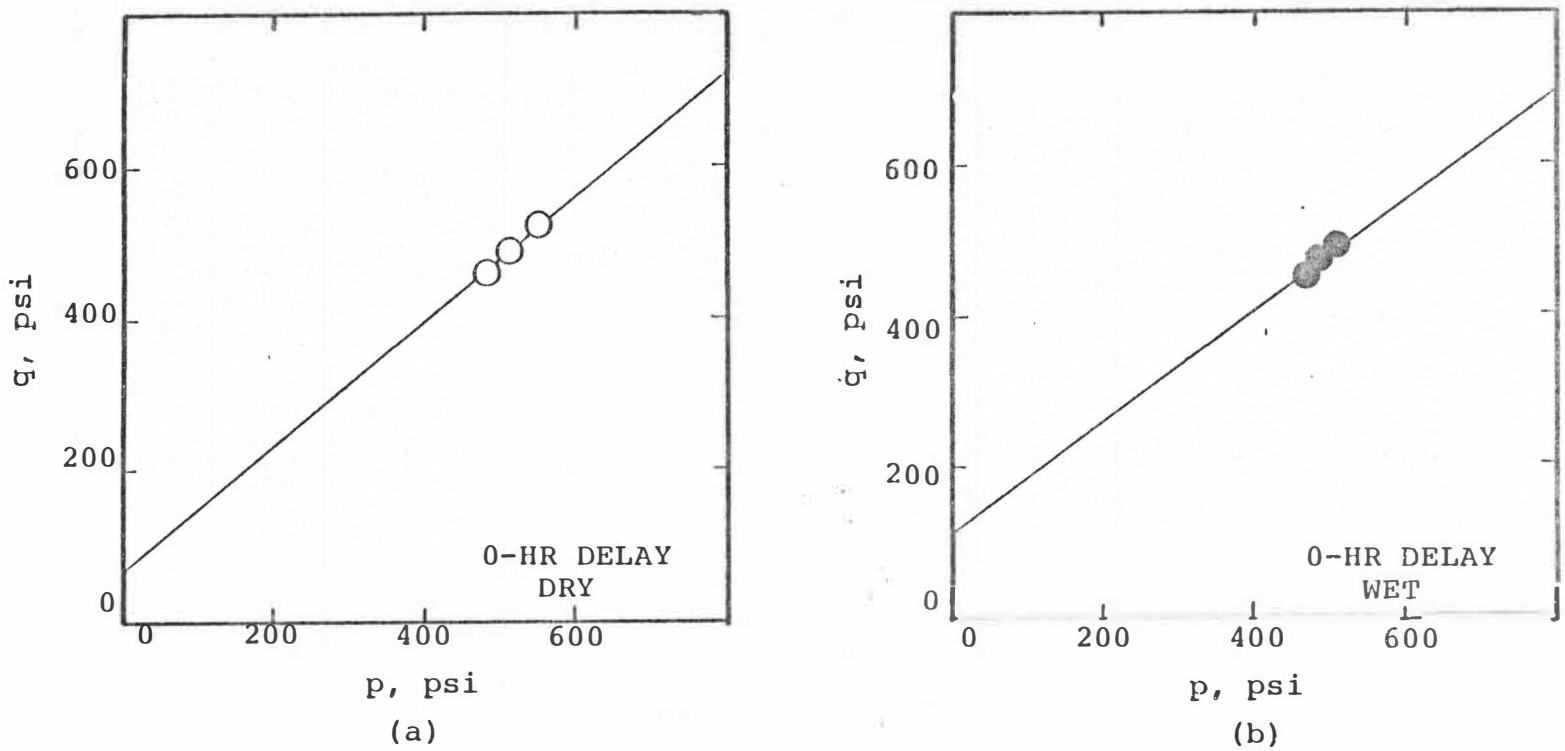

Figure A.1 Effect of wetting on the shear strength of the shale stabilized with 5% lime, cured for 28 days at 70°F and 100% relative humidity.

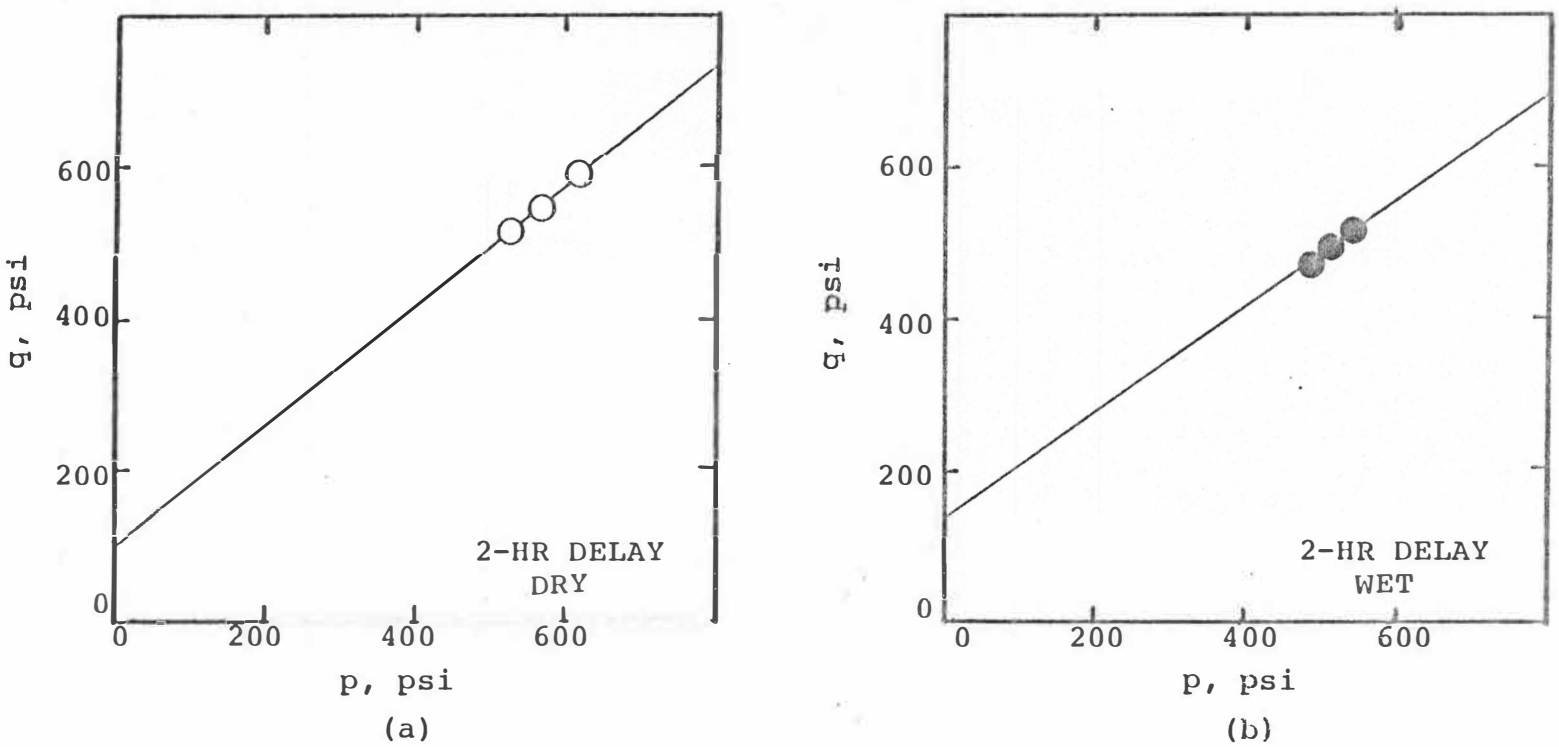

Figure A.2 Effect of wetting on the shear strength of the shale stabilized with 5% lime, cured for 28 days at 70°F and 100% relative humidity.

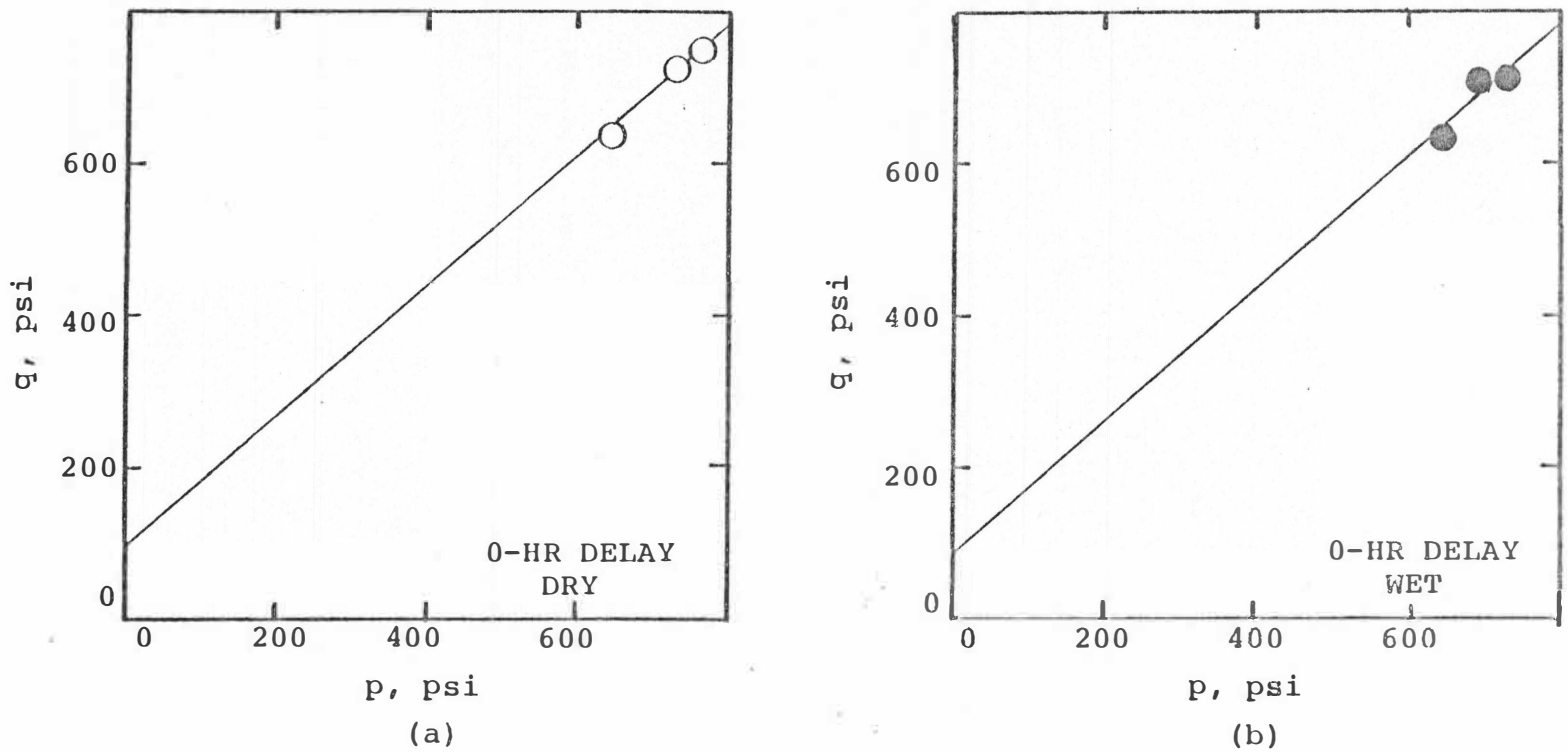

Figure A.3 Effect of wetting on the shear strength of the shale stabilized with 5% lime, cured for 28 days at 110°F and 100% relative humidity.

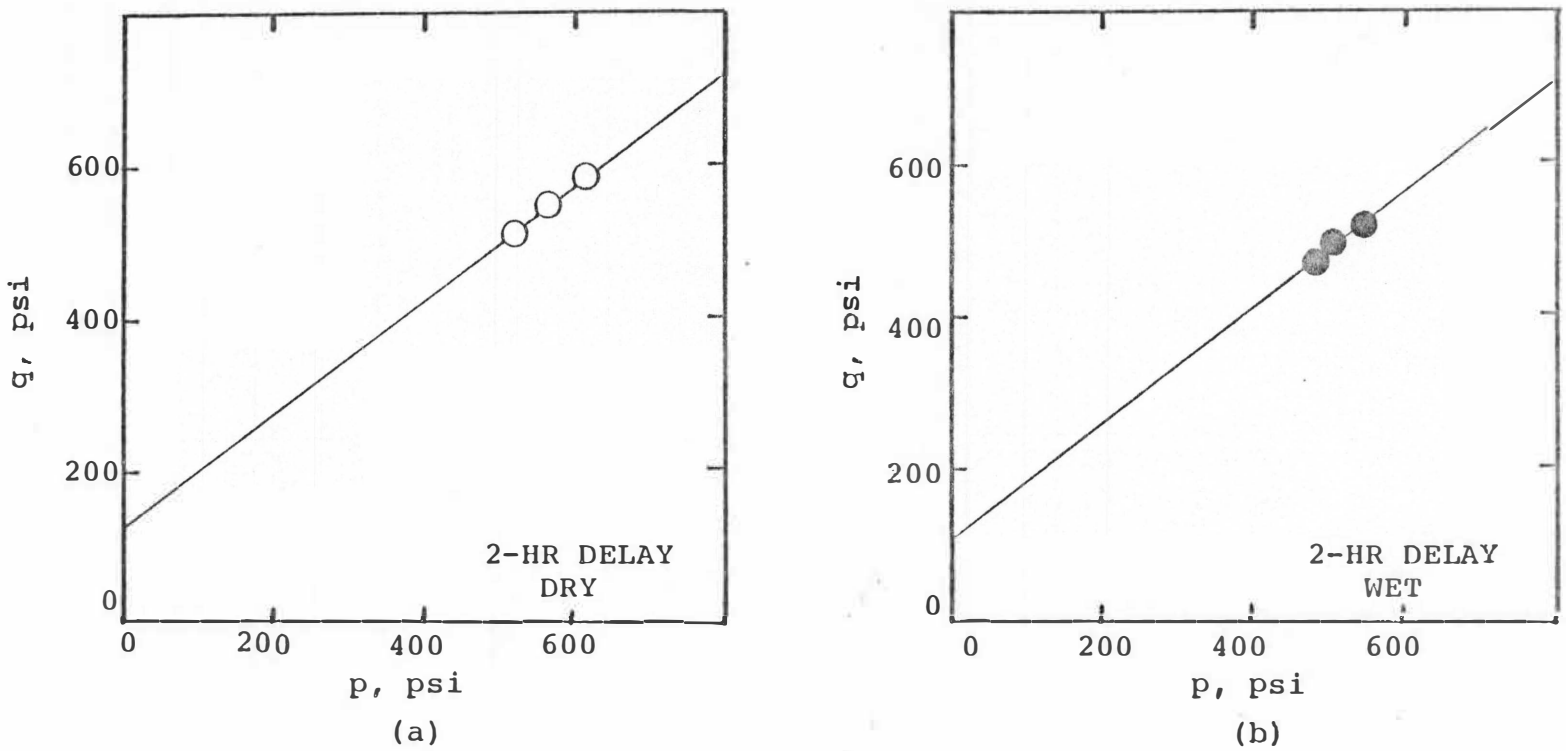

Figure A.4 Effect of wetting on the shear strength of the shale stabilized with 5% lime, cured for 28 days at 110°F and 100% relative humidity.

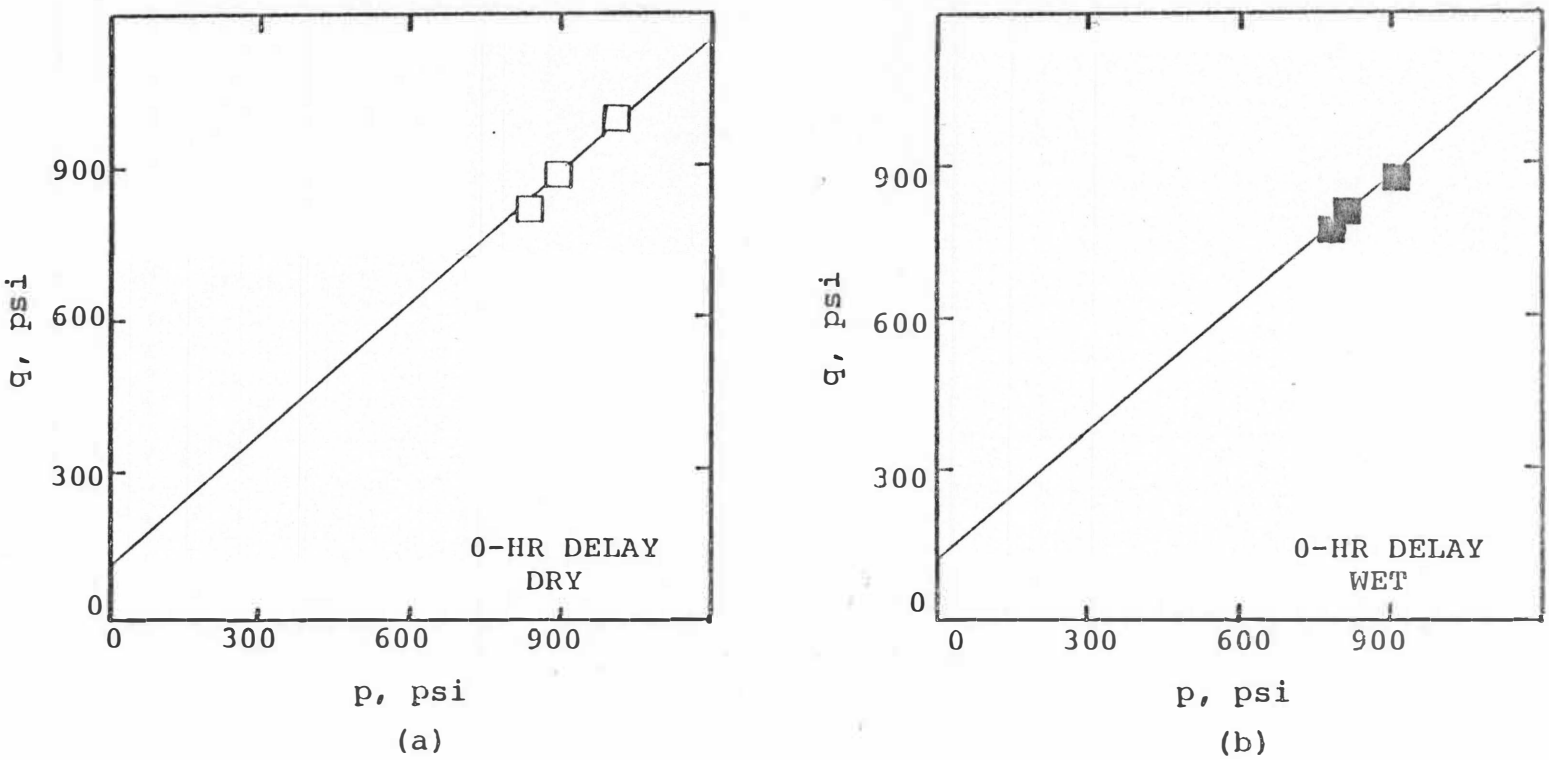

Figure A.5 Effect of wetting on the shear strength of the shale stabilized with 25% PC, cured for 28 days at 70°F and 100% relative humidity.

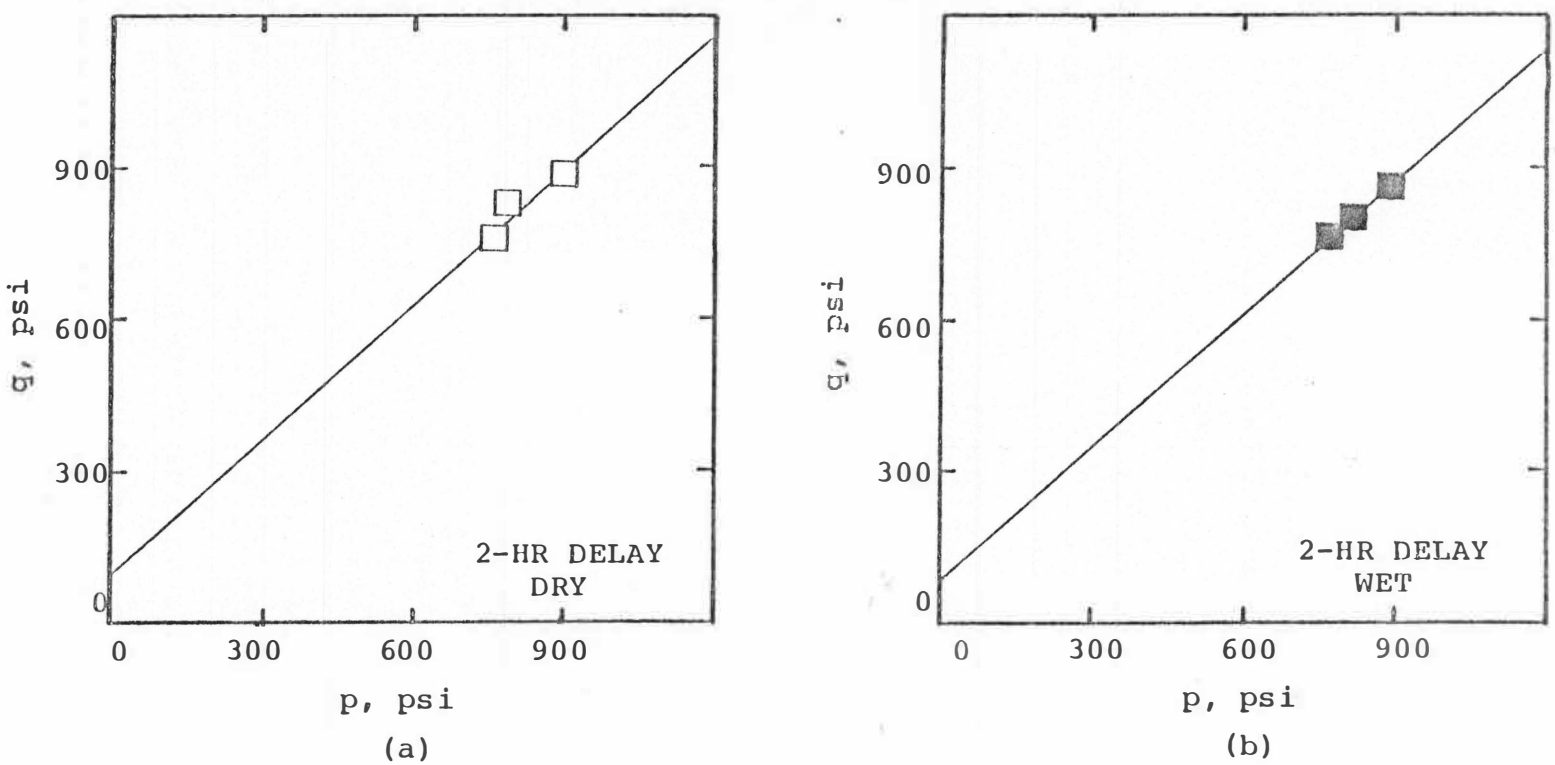

Figure A.6 Effect of wetting on the shear strength of the shale stabilized with 12% PC, cured for 28 days at 70°F and 100% relative humidity.

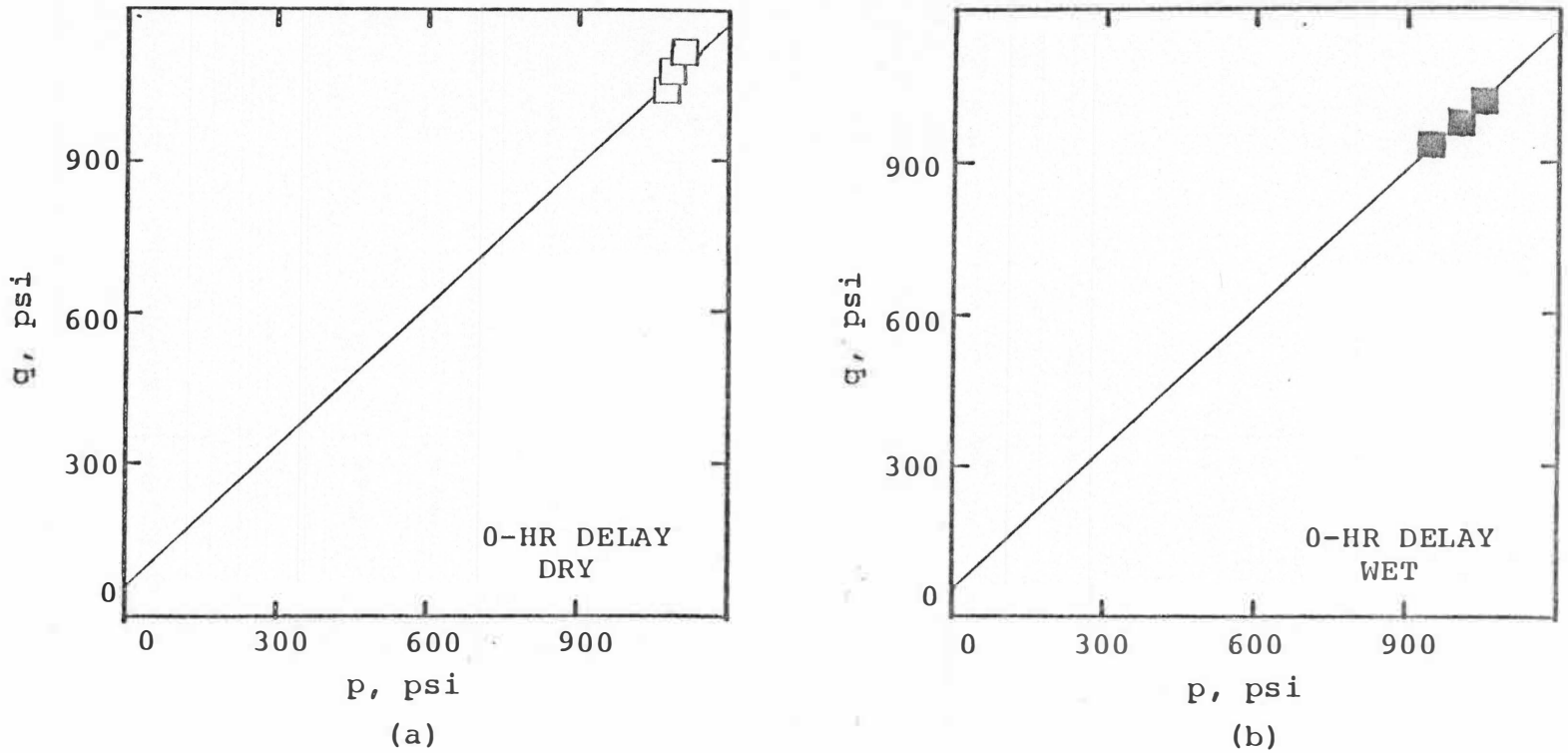

Figure A.7 Effect of wetting on the shear strength of the shale stabilized with 12% PC, cured for 28 days at 110°F and 100% relative humidity.

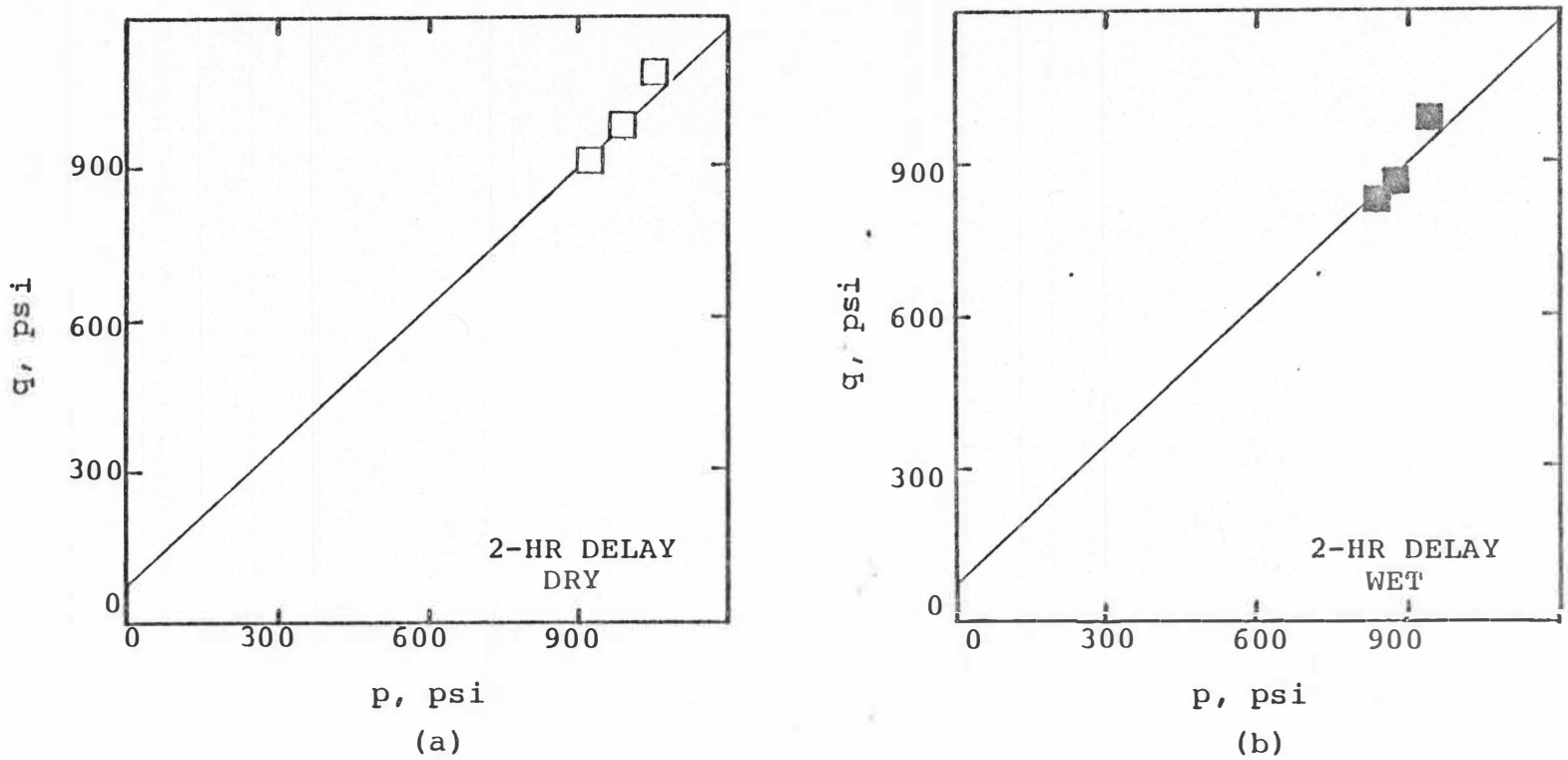

Figure A.8 Effect of wetting on the shear strength of the shale stabilized with 12% PC, cured for 28 days at 110°F and 100%relative humidity.

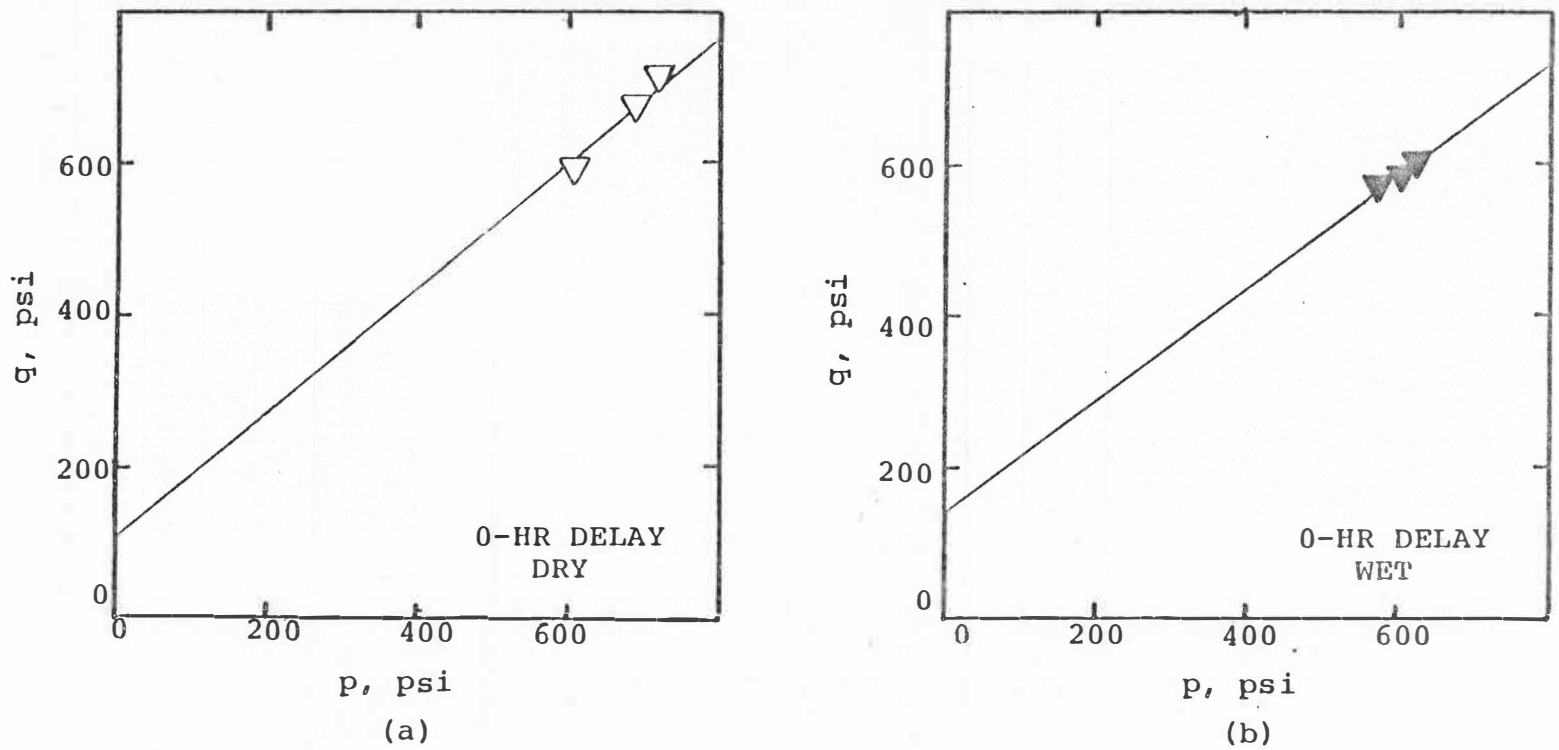

Figure A.9 Effect of wetting on the shear strength of the shale stabilized with 25% FA, cured for 28 days at 70°F and 100% relative humidity.

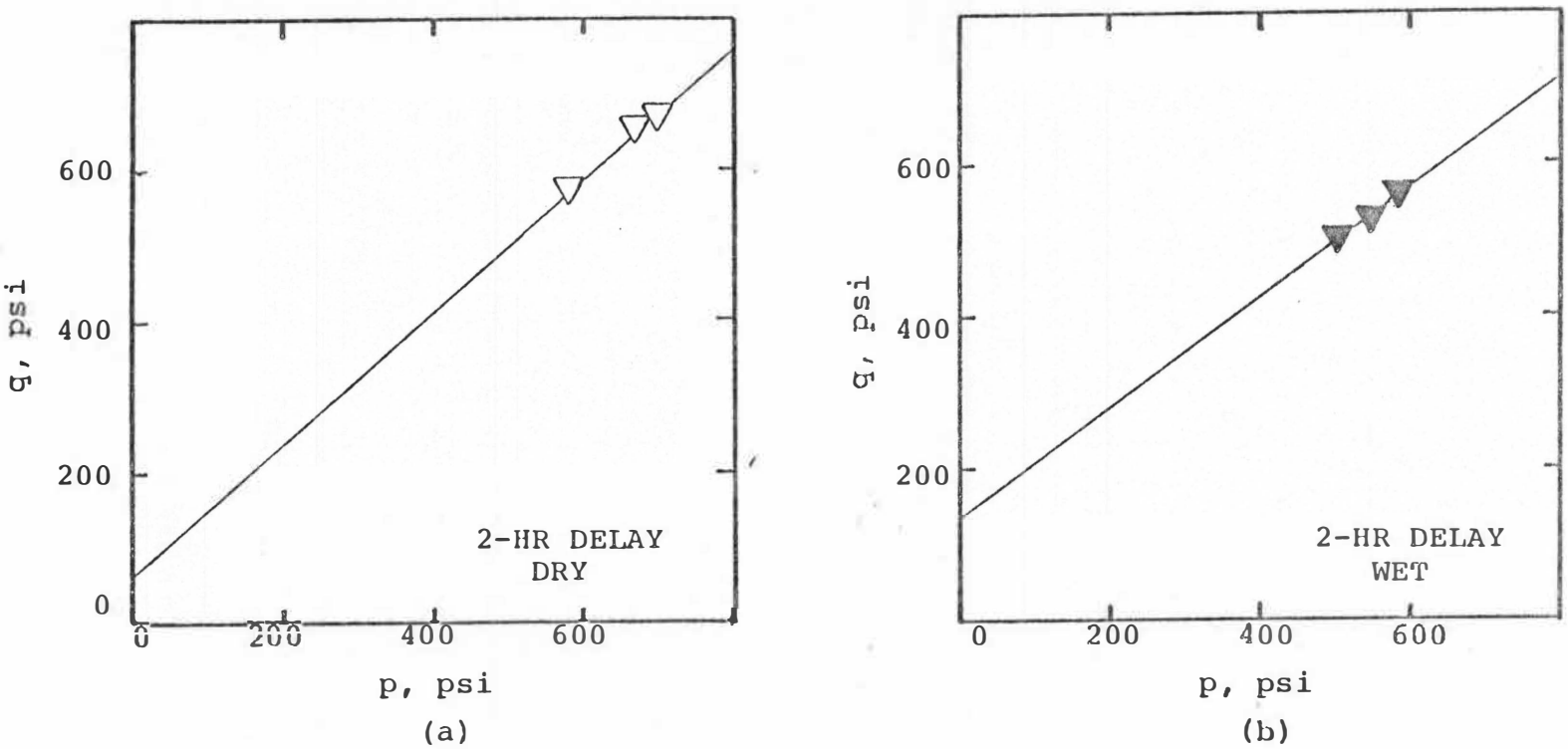

Figure A.10 Effect of wetting on the shear strength of the shale stabilized with 25% FA, cured for 28 days at 70°F and 100% relative humidity.

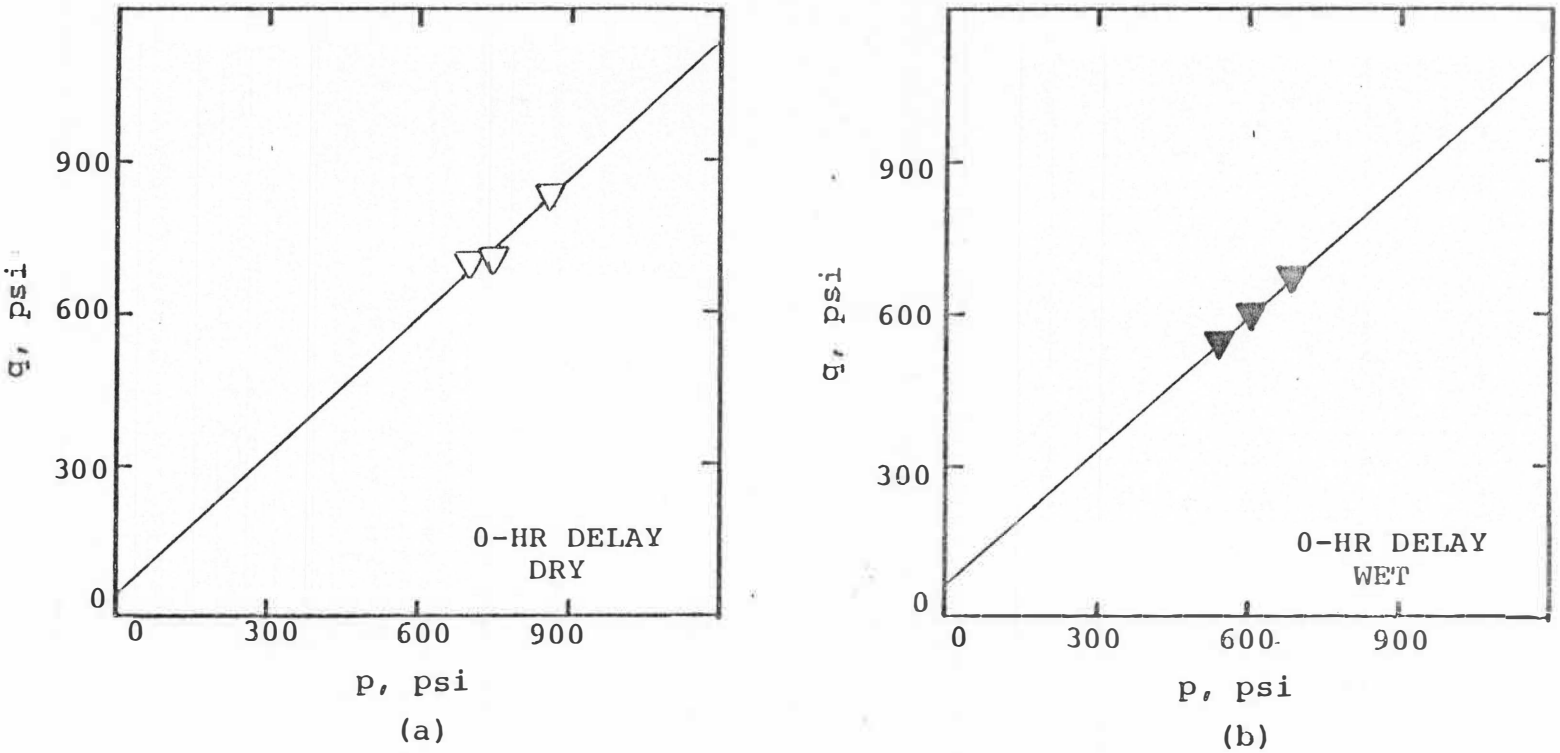

Figure A.11 Effect of wetting on the shear strength of the shale stabilized with 25% FA, cured for 28 days at 110°F and 100% relative humidity.

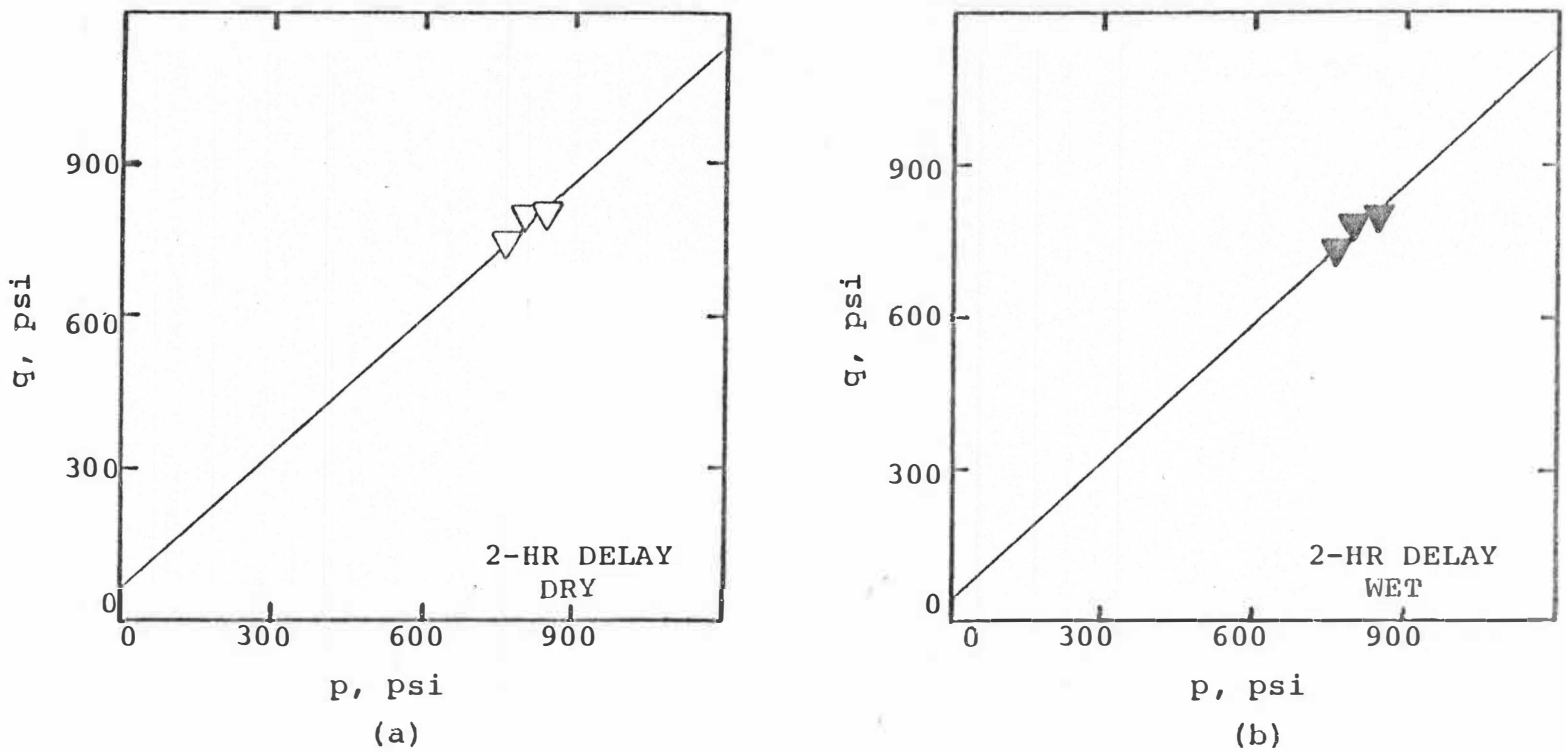

Figure A.12 Effect of wetting on the shear strength of the shale stabilized with 25% FA, cured for 28 days at 110°F and 100% relative humidity.

APPENDIX B

STRESS DIAGRAMS

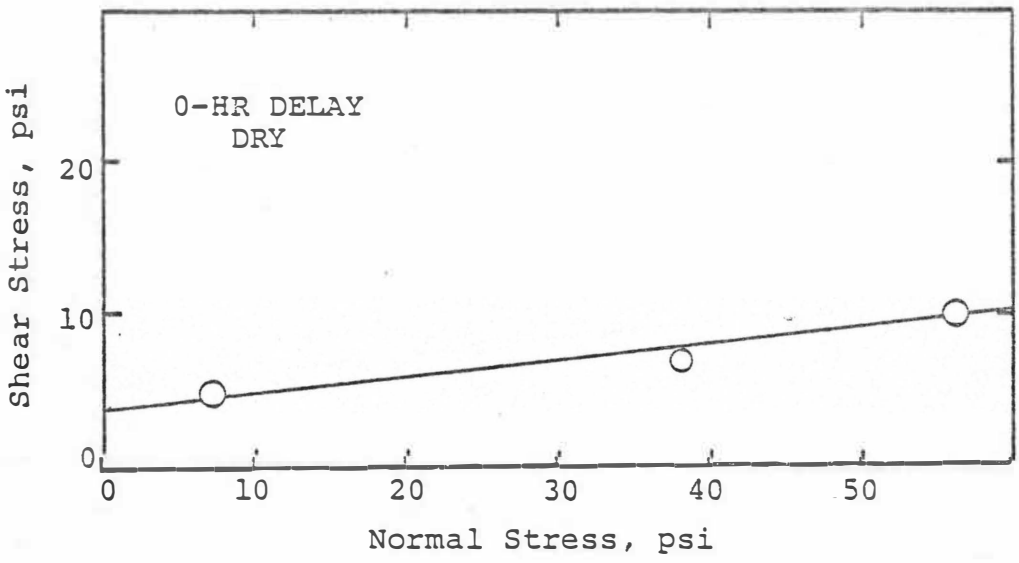

(a)

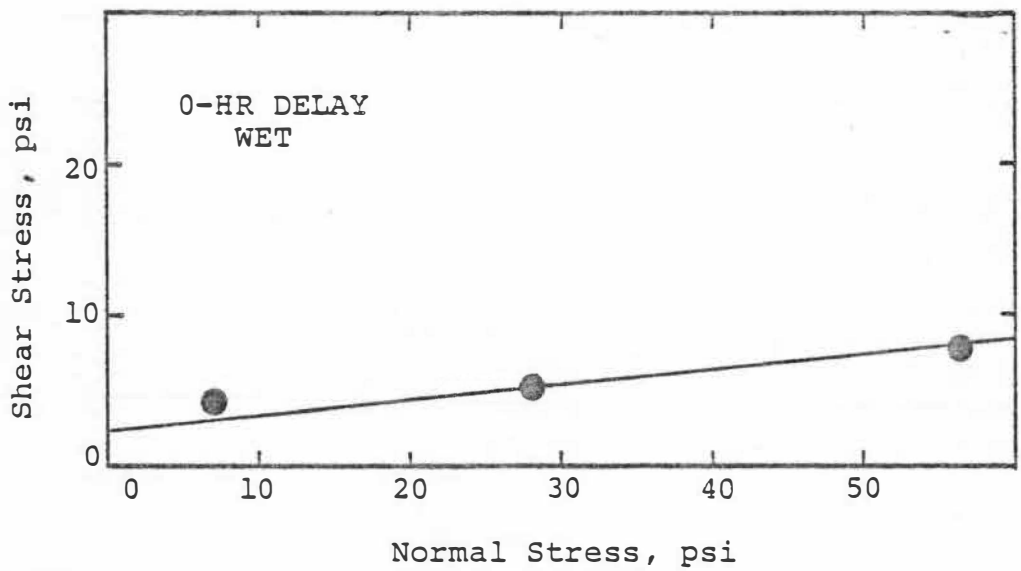

(b)

Figure B.1 Effect of wetting on the shear strength of the shale stabilized with 5% lime, cured for 28 days at 70°F and 100% relative humidity.

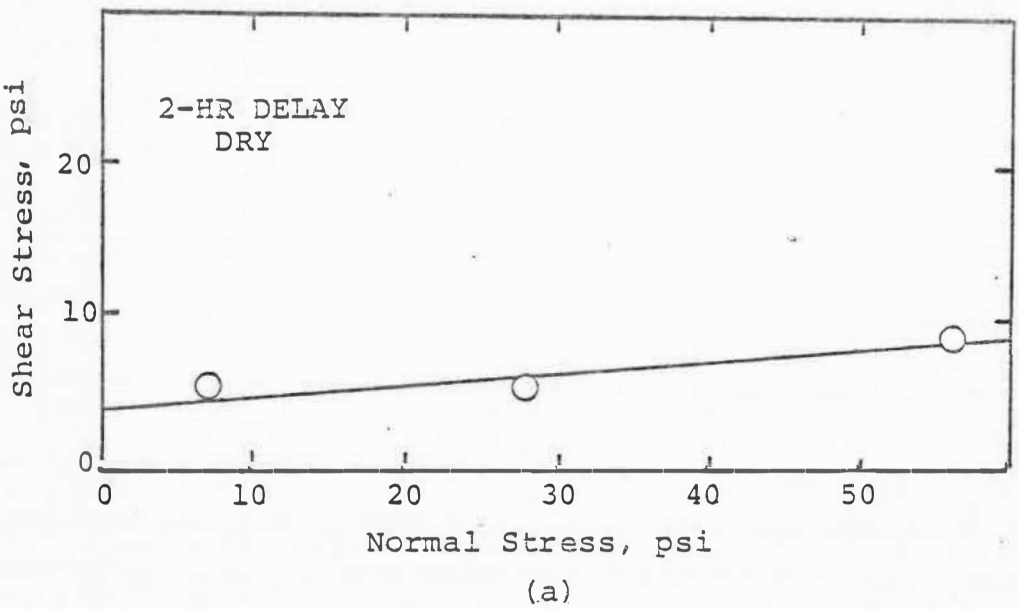

(a)

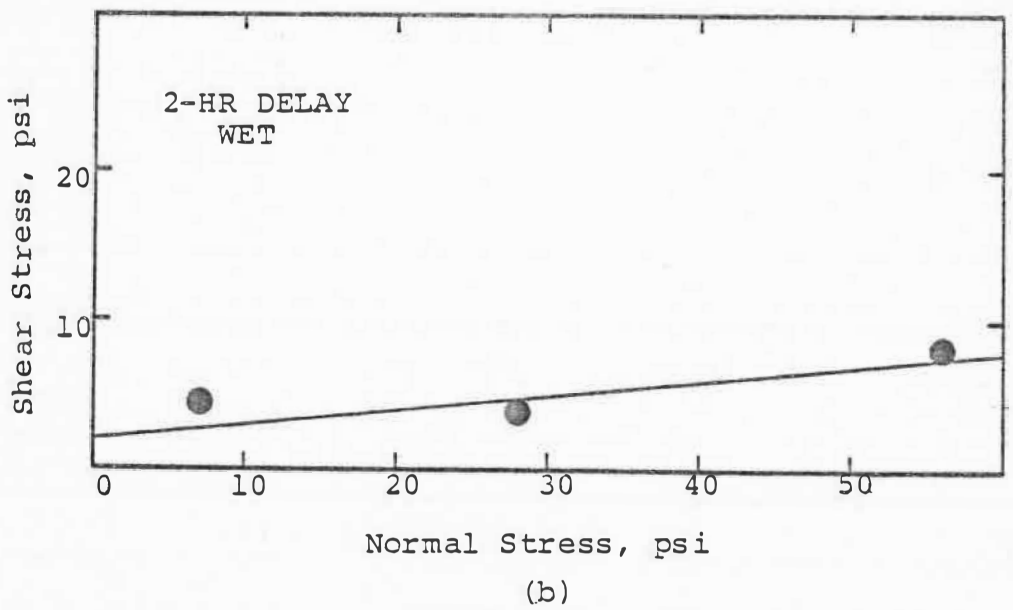

(b)

Figure B.2 Effect of wetting on the shear strength of the shale stabilized with 5% lime, cured for 28 days at 70°F and 100% relative humidity.

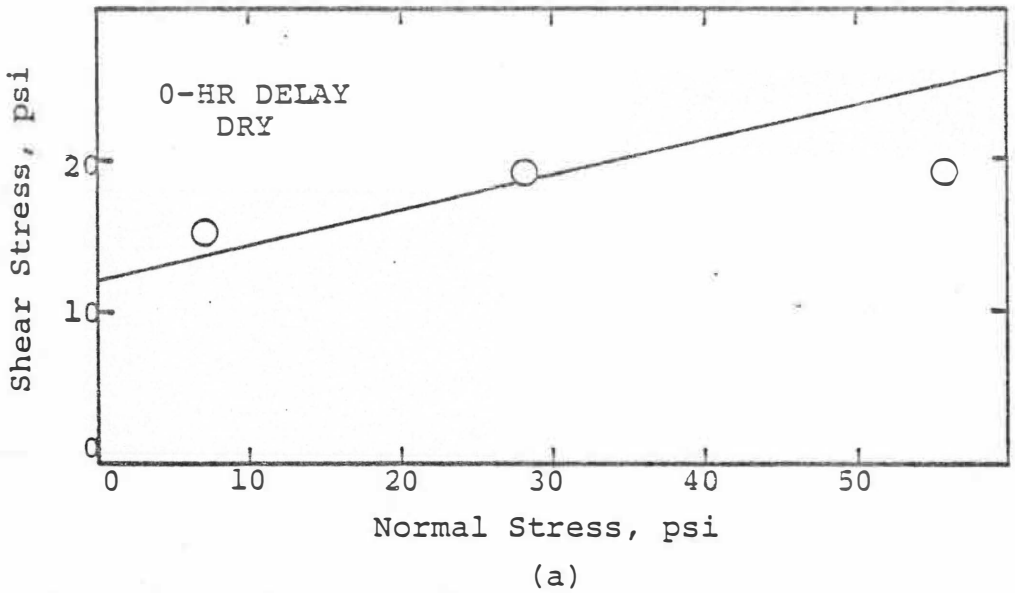

(a)

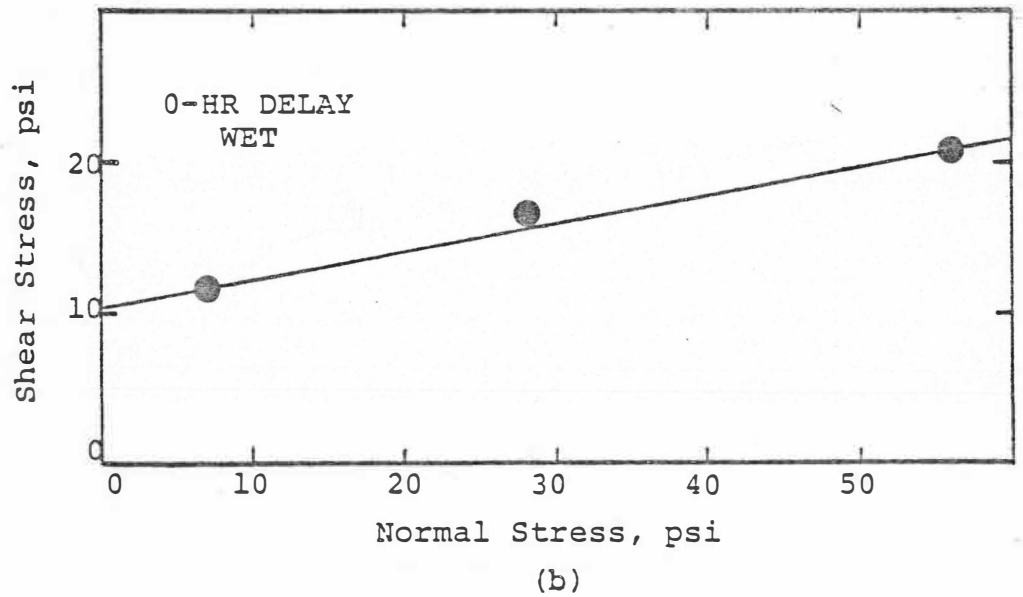

(b)

Figure B.3 Effect of wetting on the shear strength of the shale stabilized with 5% lime, cured for 28 days at 110°F and 100% relative humidity.

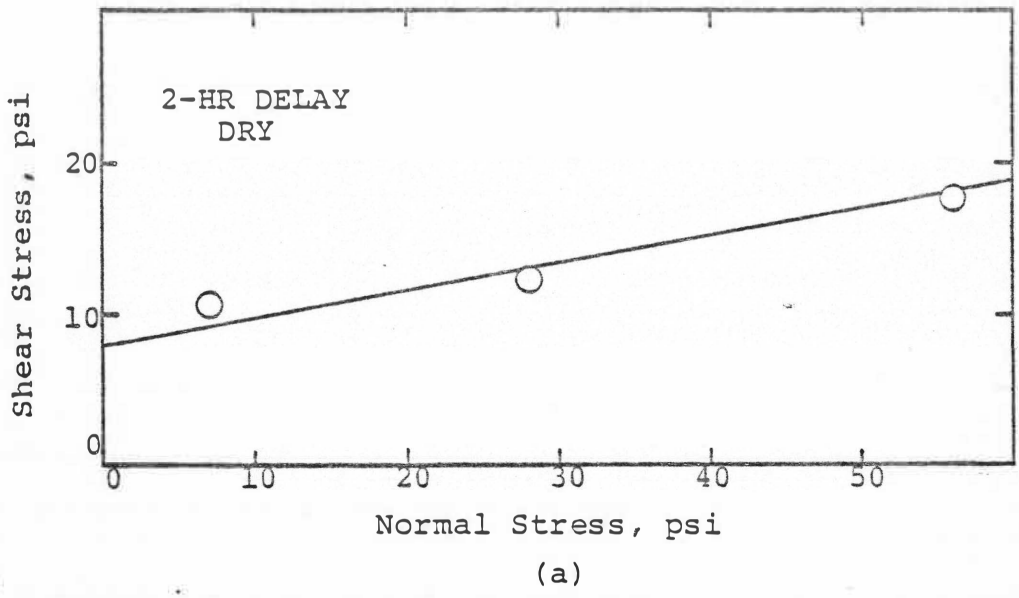

(a)

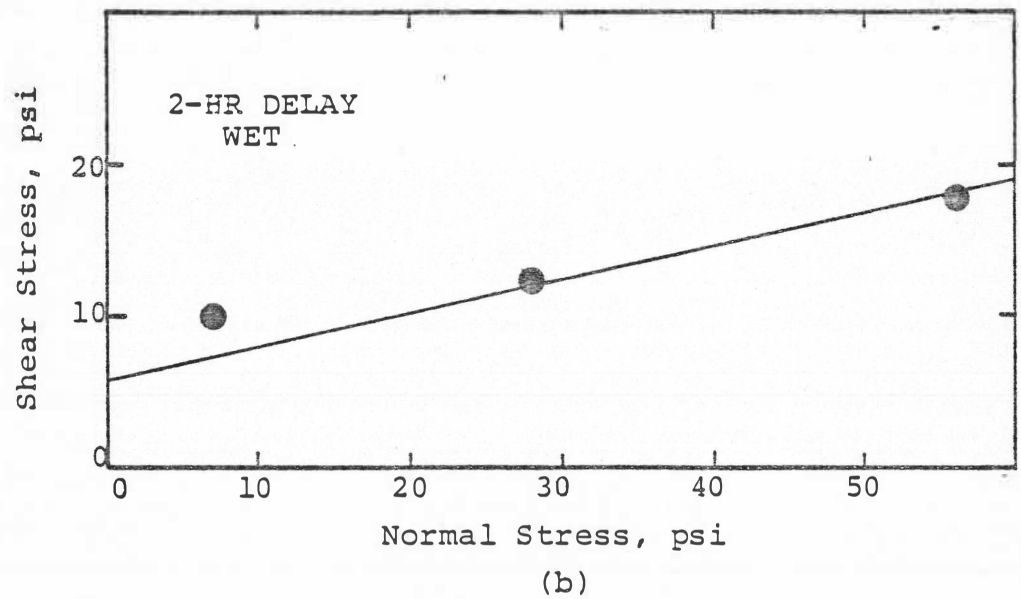

(b)

Figure 3.4 Effect of wetting on the shear strength of the shale stabilized with 5% lime, cured for 28 days at 110°F and 100% relative humidity.

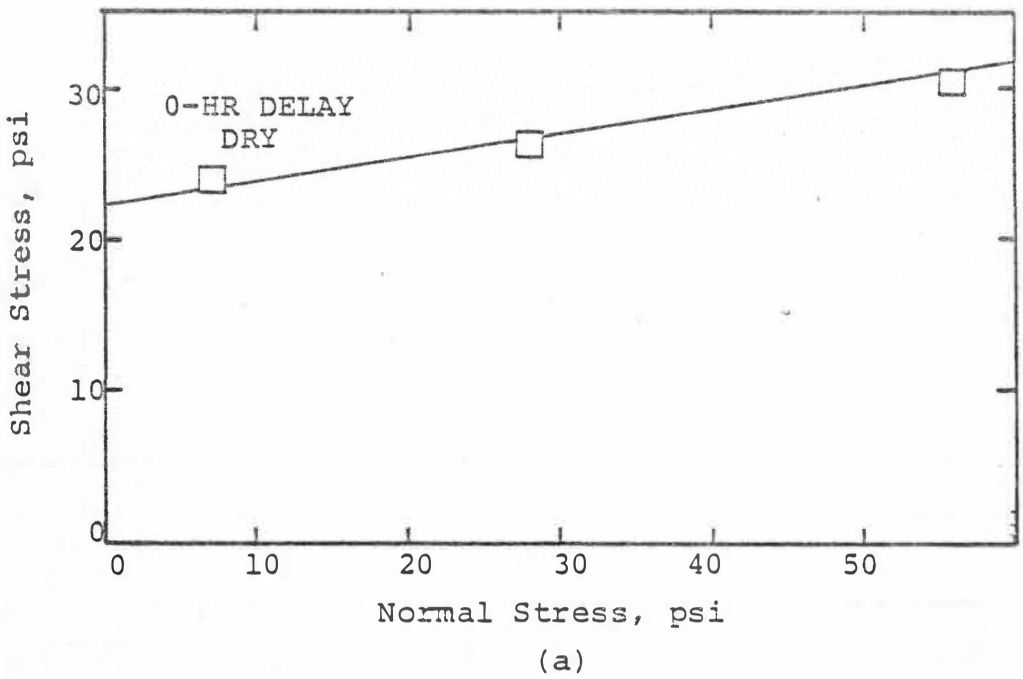

(a)

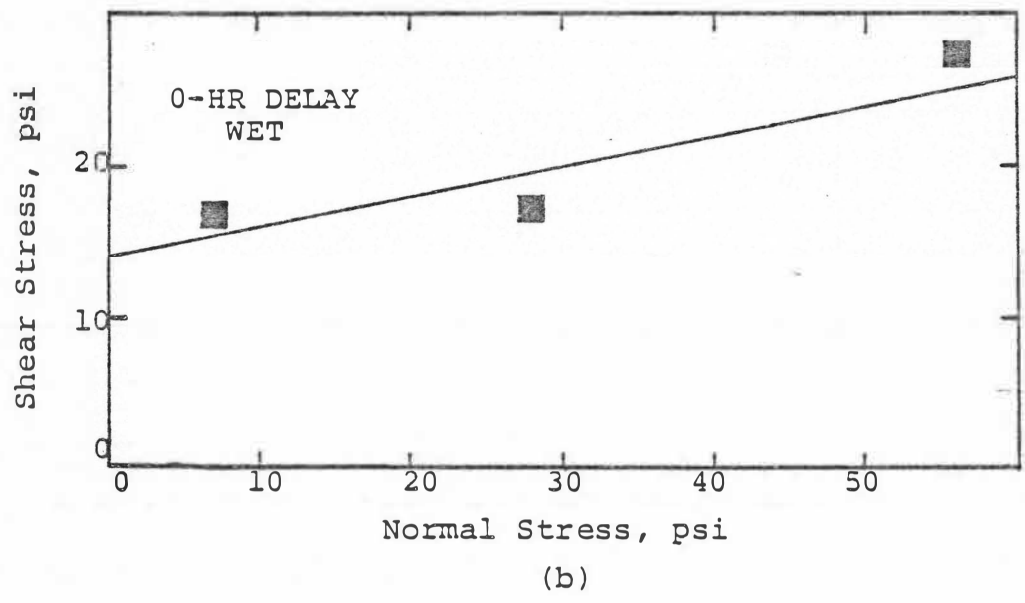

(b)

Figure B.5 Effect of wetting on the shear strength of the shale stabilized with 12% PC, cured for 28 days at 70°F and 100% relative humidity.

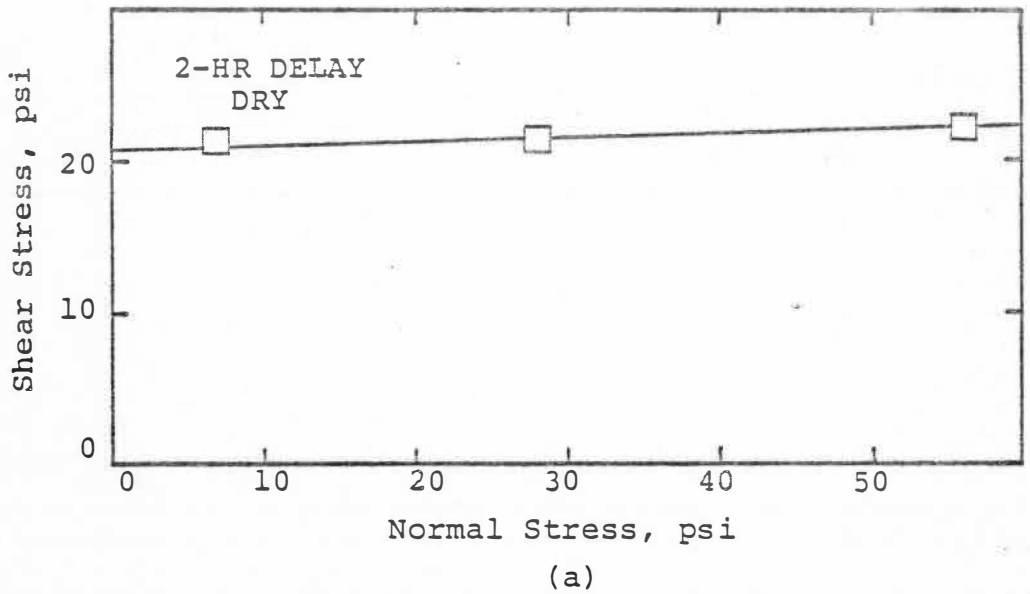

(a)

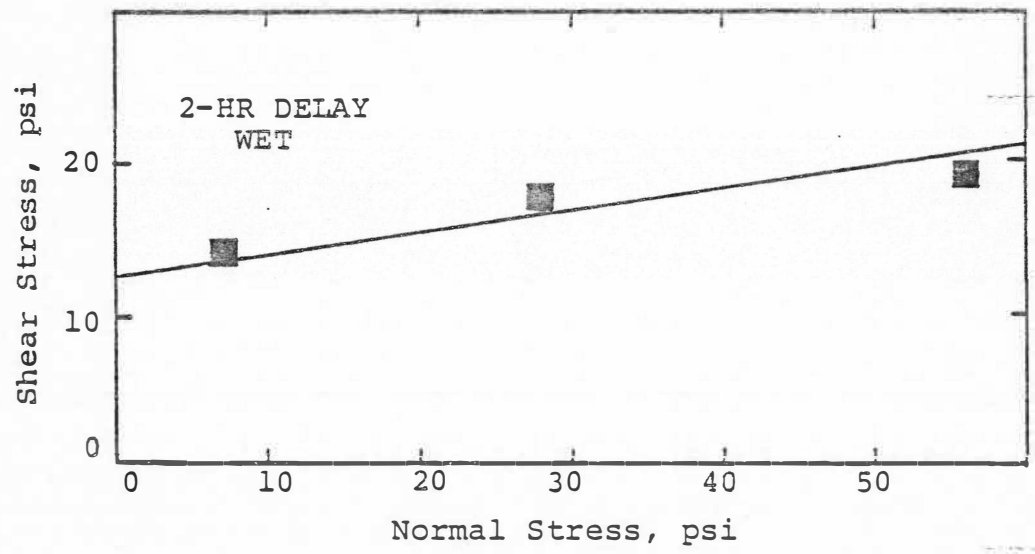

(b)

Figure B.6 Effect of wetting on the shear strength of the shale stabilized with 12% PC, cured for 28 days at 70°F and 100% relative humidity.

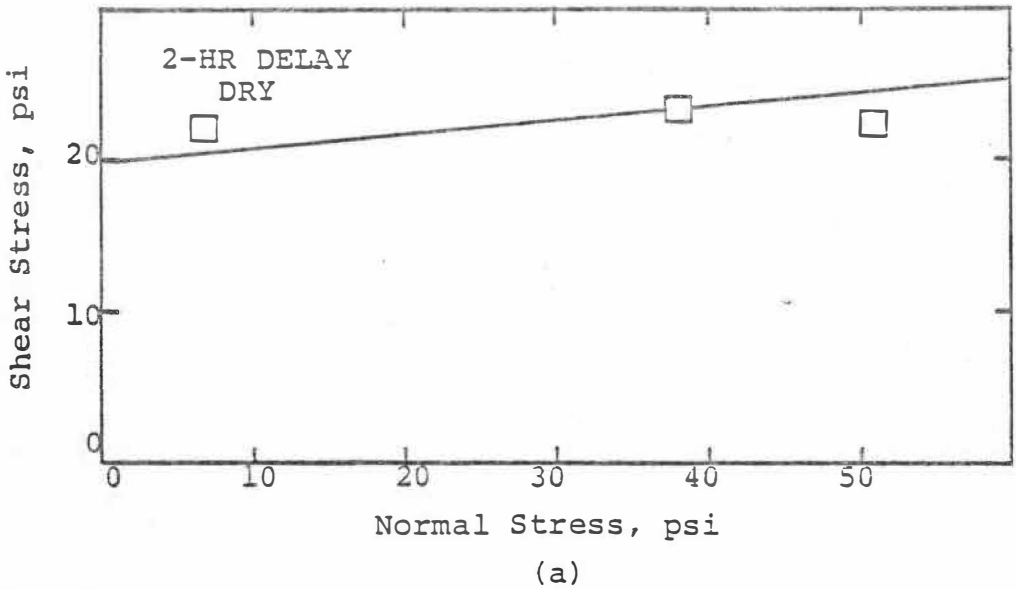

(a)

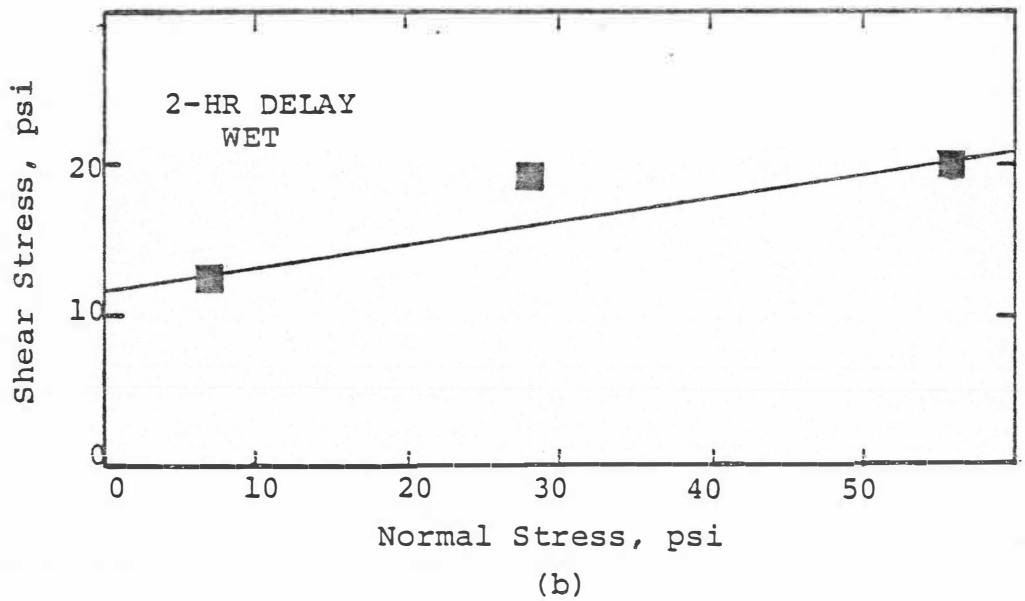

(b)

Figure B.7 Effect of wetting on the shear strength of the shale stabilized with 12% PC, cured for 28 days at 110°F and 100% relative humidity.

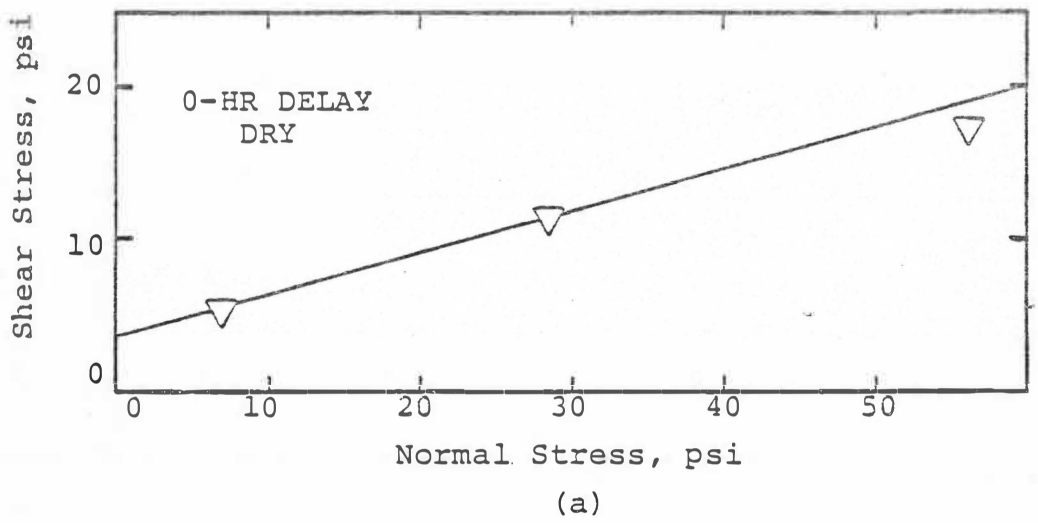

(a)

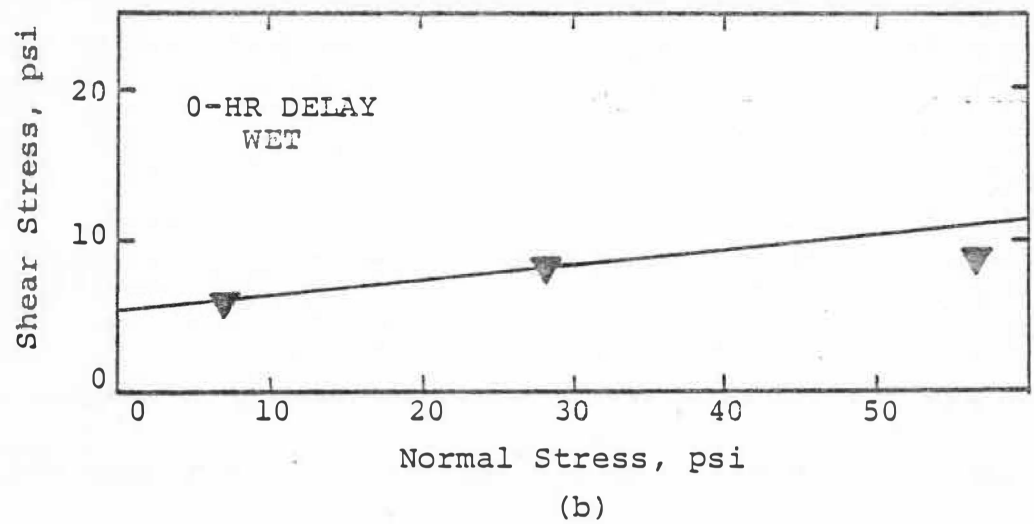

(b)

Figure B.8 Effect of wetting on the shear strength of the shale stabilized with 25% FA, cured for 28 days at 70°F and 100% relative humidity.

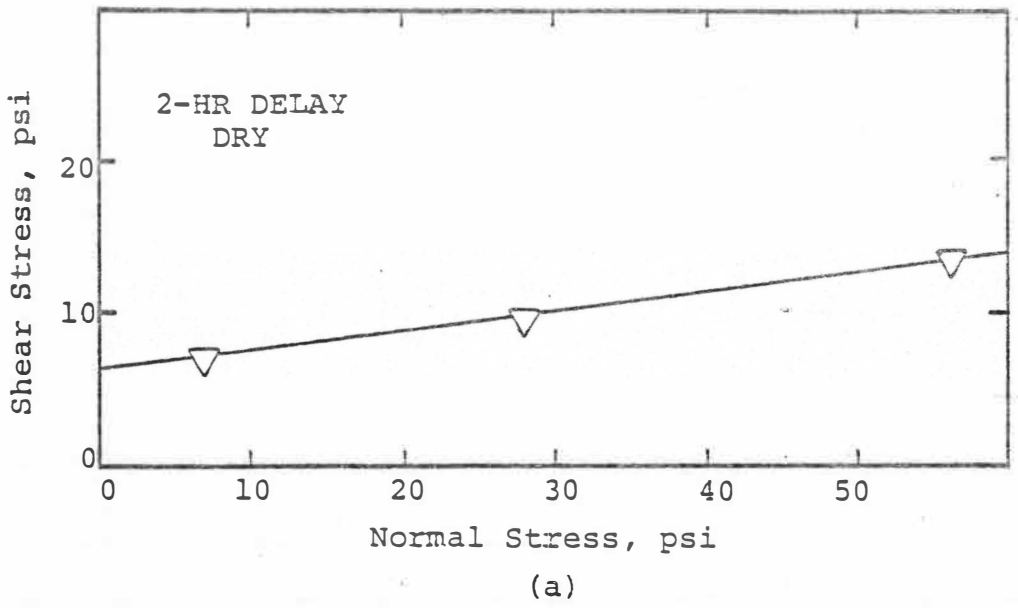

(a)

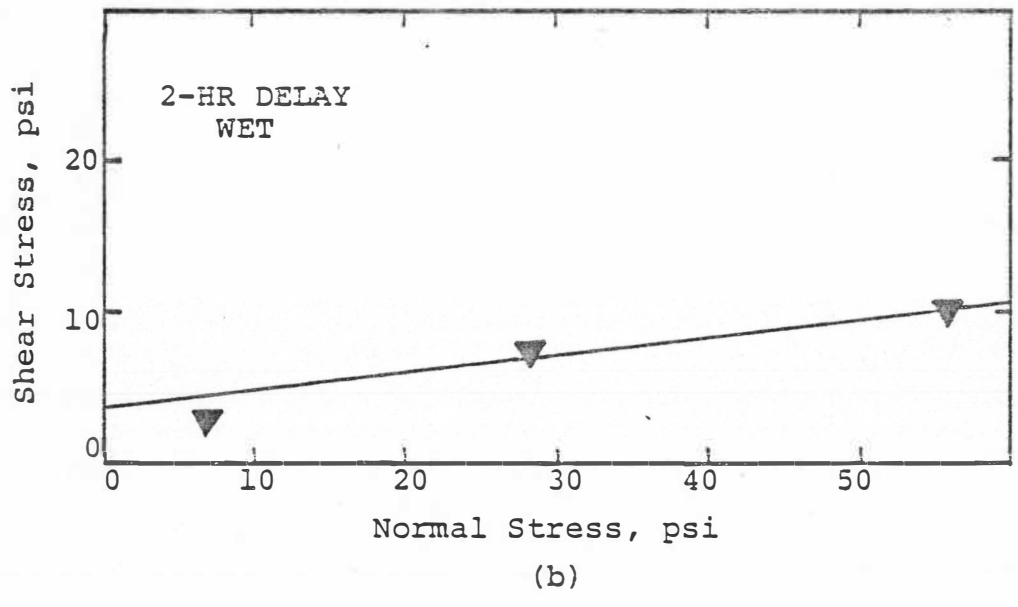

(b)

Figure B.9 Effect of wetting on the shear strength of the shale stabilized with 25% FA, cured for 28 days at 70°F and 100% relative humidity.

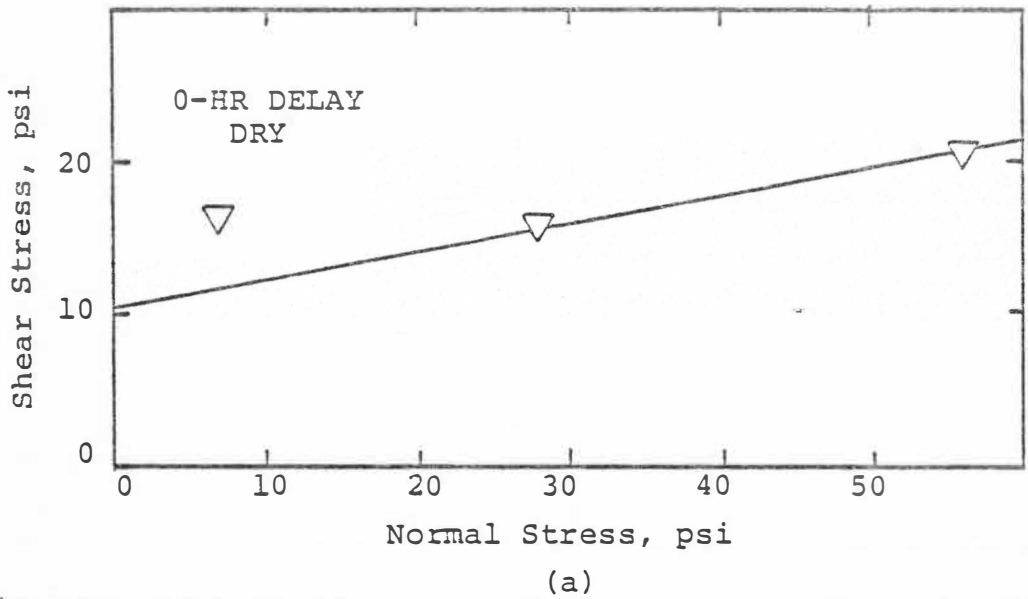

(a)

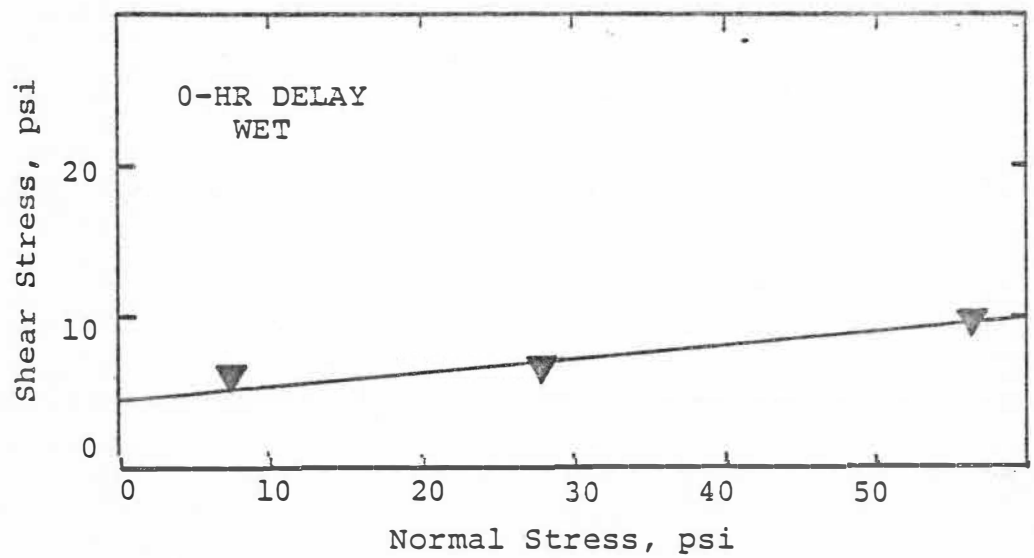

(b)

Figure B.10 Effect of wetting on the shear strength of the shale stabilized with 25% FA, cured for 28 days at 110°F and 100% relative humidity.

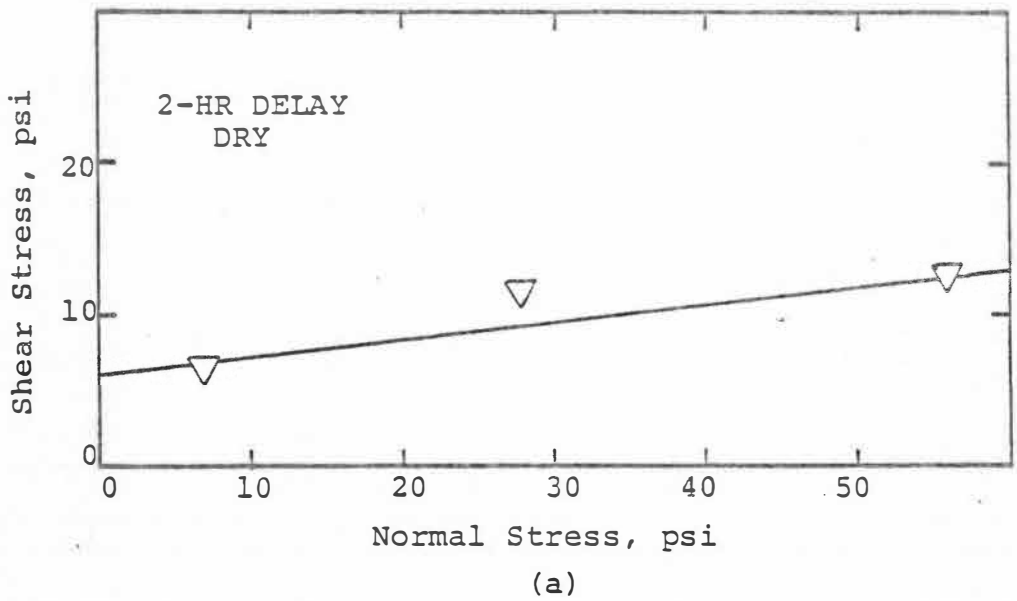

(a)

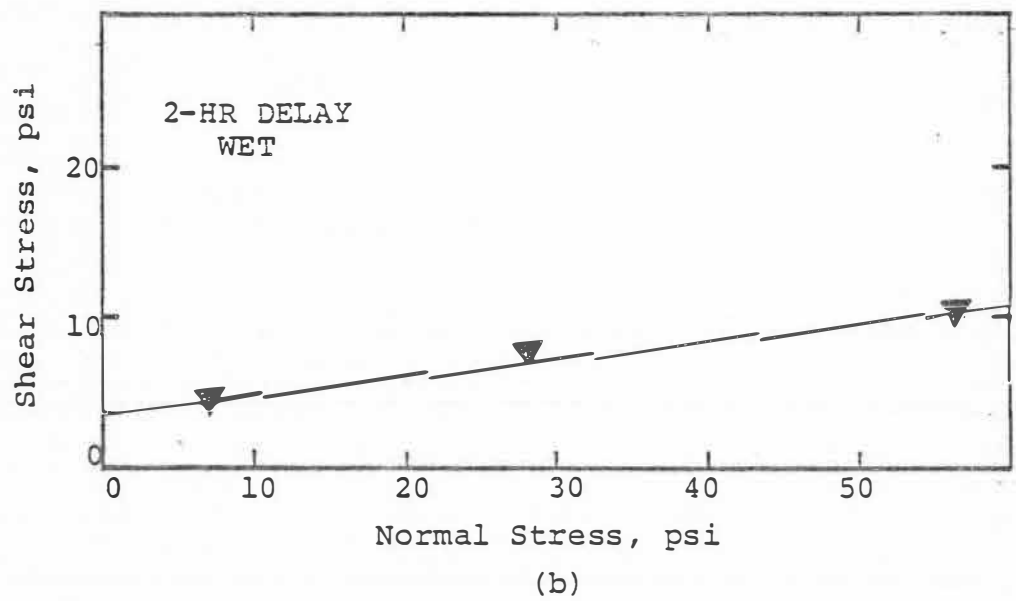

(b)

Figure B.11 Effect of wetting on the shear strength of the shale stabilized with 25% FA, cured for 28 days at 110°F and 100% relative humidity.